THE UNIVERSITY OF MICHIGAN
7577-2-Q

Technical Report ECOM-01499-1 March 1966

Azimuth and Elevation Direction Finder Study

Second Quarterly Report
1 December 1965 - 28 February 1966

Report No. 2

Contract DA 28-043-AMC-01499(E)
DA Project 5A6 79191 D902 01 04

Prepared by

D. L. Sengupta, J. E. Ferris, G. Hok, R. W. Larson and T. M. Smith

The University of Michigan Radiation Laboratory
Department of Electrical Engineering
Ann Arbor, Michigan

For

United States Army Electronics Command, Fort Monmouth, N. J.

ABSTRACT

The results of numerical computation of the radiation patterns produced by a spherical antenna array are reported. Each antenna element is assumed to produce circularly polarized radiation having a cosine type of pattern. It is found that the pattern stays fairly constant as the beam is steered over the hemisphere. For wide spacing between the elements large subsidiary lobes appear in the pattern. From the calculated patterns an estimate is made about the directivity of the array. Patterns are also calculated for the case when no phasing is introduced in the individual elements.

An approximate method is developed to explain the subsidiary lobes in the pattern produced by a circular array of isotropic elements when the spacing between the adjacent elements is of the order of or larger than a wavelength.

The basic principles of a signal processing method are described which eliminate the use of individual variable phase shifters necessary for steering the beam in conventional antenna arrays.

The results of experimental studies of the log conical spiral antenna and a VHF power dividing circuit are reported.

FOREWORD

This report was prepared by The University of Michigan Radiation Laboratory of the Department of Electrical Engineering under United States Army Electronics Command Contract No. DA 28-043 AMC-01499(E). This contract was initiated under United States Army Project No. 5A6 79191 D902 01 04 "Azimuth and Elevation Direction Finder Study". The work is administered under the direction of the Electronics Warfare Division, Advanced Techniques Branch at Fort Monmouth, New Jersey. Mr. S. Stiber is the Project Manager and Mr. E. Ivone is the Contract Monitor.

The material reported herein represents the results of the preliminary investigation into the study of the feasibility of designing a broadband circularly polarized direction finder antenna with hemispherical coverage.

TABLE OF CONTENTS

LIST OF ILLUSTRATIONS

I
INTRODUCTION

This is the second report on a study to determine the possibility of developing a broadband VHF azimuth and elevation direction finder. In the first report (Sengupta, et al, 1965) we discussed theoretically the possibility of using an antenna array consisting of individual elements placed on the surface of a sphere. The present report discusses in more detail the different aspects of the radiation characteristics of such a spherical array. The plan of the report is as follows.

Chapter II deals with the radiation patterns produced by antennas placed on the surface of a sphere. It is assumed that each antenna element produces circularly polarized variation. With an assumed expression for the individual pattern, the general expression for the radiation pattern as given in the previous report is recast into a form suitable for numerical computation. Calculated radiation patterns in two orthogonal planes and for different scan angles are given. The effects of increasing the diameter of the sphere (which increases the spacing between the elements) on the radiation patterns are also investigated. It is found that for wide spacing between the adjacent elements large subsidiary lobes appear in the pattern. A few patterns are given for the case when no phasing is introduced into the individual elements. The chapter closes with a discussion on the expected directivity of the array.

In Chapter III an attempt is made to understand the behavior of large subsidiary lobes in the pattern produced by an array when the elements are widely spaced on a curved surface. The model chosen for the study is a circular array of isotropic elements with the spacing between the adjacent elements being of the order of or larger than a wavelength. We have developed an approximate procedure to predict the dominant subsidiary maxima in the patterns. It is hoped that the results of the investigation will be of use in understanding the case when the antenna elements are widely spaced on a curved surface.

The bulk and inertia of microwave and VHF phase shifters have stimulated an investigation of a signal processing method which does not require an individual variable phase delay for each antenna element. Chapter IV describes briefly the principle of such a system which eliminates the phase shifters at the cost of a certain loss in signal-to-noise ratio.

Chapter V gives the results of some experimental work. The results of a study of the VSWR properties of a log conical spiral antenna are given. A VHF power dividing circuit is developed for feeding a number of elements from a single transmission line. Its performance is discussed briefly.

II

RADIATION CHARACTERISTICS OF THE SPHERICAL ARRAY

The radiation characteristics of a spherical antenna array are discussed in this chapter. The array consists of circularly polarized antenna elements placed on the surface of a sphere. The radiation pattern expressions for such an array are discussed briefly at first. Numerically computed patterns produced under different cases are then discussed. On the basis of the calculated patterns the expected directivity of such a type of array is also discussed.

2.1 Theoretical Expressions for the Radiation Pattern

The theoretical basis of analyzing the radiation patterns produced by a spherical antenna array has been discussed (Sengupta, et al, 1965). It was shown that the complete expression for the total electric field $\vec{E}(\theta, \phi)$ produced at the far field point $P(R, \theta, \phi)$ by an array of antenna elements placed on the surface of a sphere of radius a, is given by

$$\vec{E}(\theta, \phi) = \sum_n \sum_m \delta_{nm} \vec{E}_{nm}(\theta', \phi') e^{ika \cos \theta'} \quad , \tag{2.1}$$

where the factor $e^{i(\omega t - kR)}/R$ has been omitted. The notations used in eq. (1) are:

the fixed coordinate system (θ, ϕ) and the dummy system (θ', ϕ') were as discussed in the First Quarterly Report ,

$$\cos \theta' = \sin \alpha_n \sin \theta \cos(\phi - \beta_{nm}) + \cos \alpha_n \cos \theta \quad , \tag{2.2}$$

α_n, β_{nm} are the coordinates of an antenna element on the spherical surface; they are determined by the particular choice of element distribution,

δ_{nm} is a conditional on-off switch which will be discussed later,

$\vec{E}_{nm}(\theta', \phi')$ is the element pattern to be discussed below,

$k = 2\pi/\lambda$ is the propagation constant.

Each antenna element is assumed to produce circularly polarized radiation fields. The individual antenna field is assumed to be given by

$$\vec{E}_{nm}(\theta', \phi') = (\hat{e}_{\theta'} - i\hat{e}_{\phi'}) \cos\theta' \, e^{-i\phi'} \quad , \tag{2.3}$$

where $\hat{e}_{\theta'}$ and $\hat{e}_{\phi'}$ are unit vectors in the corresponding directions. In (2.3) the angle θ' is restricted to the range $-\pi/2 \leqslant \theta' \leqslant \pi/2$. This means that the individual pattern is a unidirectional cosine type. A pair of crossed dipoles excited in phase quadrature and placed $\lambda/4$ above a conducting ground plane will produce a field pattern which is approximately given by (2.3). Helical and log-conical antenna radiation patterns may also be approximated by (2.3) under some special circumstances. Equation (2.3) may also be expressed in (θ, ϕ) coordinates as follows:

$$\vec{E}_{nm}(\theta', \phi') = -(\hat{e}_{\theta} - i\hat{e}_{\phi}) \cos\theta' \, e^{-i(\phi' + \nu_{nm})} \quad , \tag{2.4}$$

where $\cos\theta'$ is given in (2.2),

$$\tan\phi' = \frac{\sin\theta \sin(\phi - \beta_{nm})}{\sin\theta \cos\alpha_n \cos(\phi - \beta_{nm}) - \cos\theta \sin\alpha_n} \tag{2.5}$$

$$\tan\nu_{nm} = \frac{\sin\alpha_n \sin(\phi - \beta_{nm})}{\sin\alpha_n \cos\theta \cos(\phi - \beta_{nm}) - \cos\alpha_n \sin\theta} \quad . \tag{2.6}$$

Let $\xi_{nm} = \phi' + \nu_{nm}$. Then it can be shown that

$$\tan \xi_{nm} = \frac{(\cos \alpha_n + \cos\theta)\sin(\phi - \beta_{nm})}{\sin\alpha_n \sin\theta + (\cos\theta\cos\alpha_n + 1)\cos(\phi - \beta_{nm})} \quad . \tag{2.7}$$

Thus, (2.1) can be written as

$$\vec{E}(\theta,\phi) = -(\hat{e}_\theta - i\hat{e}_\phi)A(\theta,\phi) \quad , \tag{2.8}$$

where

$$A(\theta,\phi) = \sum_n \sum_m \delta_{nm}\psi_{nm} e^{i\left[ka\psi_{nm} - \xi_{nm}\right]} \quad , \tag{2.9}$$

where $\psi_{nm} = \cos\theta'$. In (2.8) $\left|A(\theta,\phi)\right|$ may be looked upon as the pattern produced by the array.

If the antenna elements are phased such that the pattern produces a maximum in the direction θ_o, ϕ_o, then the pattern expression should be modified into

$$A(\theta,\phi) = \sum_n \sum_m \delta_{nm}\psi_{nm} e^{i\left[ka(\psi_{nm} - \Delta_{nm}) - (\xi_{nm} - \eta_{nm})\right]} \quad , \tag{2.10}$$

where

$$\Delta_{nm} = \psi_{nm}(\theta_o, \phi_o) = \cos\theta_o\cos\alpha_n + \sin\theta_o\sin\alpha_n\cos(\phi_o - \beta_{nm}) \quad , \tag{2.11}$$

$$\eta_{nm} = \xi_{nm}(\theta_o, \phi_o) = \tan^{-1}\left[\frac{\sin\alpha_n\sin(\phi_o - \beta_{nm})}{\sin\alpha_n\cos\theta_o\cos(\phi_o - \beta_{nm}) - \cos\alpha_n\sin\theta_o}\right] \quad . \tag{2.12}$$

A detailed description of the element distribution may be found in the first quarterly report (Sengupta, et al, 1965).

The quantities governing the distribution are

$$\alpha_n = 90^o - n\,15^o \quad , \tag{2.13}$$

$$\beta_{nm} = \frac{72^o m}{6 - |n|} \tag{2.14}$$

with the exceptions $\beta_{0m}=\beta_{1m}$ and $\beta_{6m}=0$ and where $-6\leq n\leq 6$ and m is an integer ranging from 0 to values as high as 25 depending on n.

2.2 Calculated Patterns of the Spherical Array

When the element distribution given by (2.13) and (2.14) is introduced to the array factor in (2.10) we obtain

$$A(\theta,\phi)=\sum_{n=-6}^{6}\sum_{m=0}^{M(n)}\delta_{nm}\psi_{nm}e^{i\left[ka(\psi_{nm}-\Delta_{nm})-(\xi_{nm}-\eta_{nm})\right]} \qquad (2.15)$$

where

$$M(n)=5(6-|n|)-1, \text{ for } n=\pm 1,\pm 2,\pm 3,\pm 4,\pm 5$$
$$M(\pm 6)=0$$
$$M(0)=M(1).$$

The value of M(n) is found from (2.14) and the two exceptions, β_{0m} and β_{6m}, govern M(0) and $M(\pm 6)$.

The on-off condition switch δ_{nm} is controlled by the factors ψ_{nm} and Δ_{nm}. For a hemisphere aperture distribution centered at θ_o, ϕ_o

$$\delta_{nm}=\begin{cases}1, & \text{if } \Delta_{nm}>0 \text{ and } \psi_{nm}\geq 0\\ 0, & \text{otherwise}\end{cases}. \qquad (2.16)$$

Physically, in (2.16), $\psi\geq 0$ means that only those elements which are visible from point θ,ϕ contribute to the sum in (2.15). The quantity $\Delta_{nm}>0$ means that only those elements which lie within 90^o of the point θ_o,ϕ_o contribute to (2.15). The size of the activated aperture is controlled by Δ_{nm}. Another example of an activated aperture is $\Delta_{nm}>.86$ which is an aperture that covers 30^o in all directions from point (θ_o,ϕ_o). It is noted that the physical meaning of Δ_{nm} and ψ_{mn} in (2.16) is completely independent of their meaning in (2.15) even though they are the same parameters.

Equation (2.15) has been computed in two orthogonal planes. Cut I is the polar plane which always passes through $\theta=0^o$ and is determined by

$$\phi=\phi_o$$
$$\theta=\theta_o+p\,5^o \qquad p = 0, 1, 2, \ldots, 72 \qquad (2.17)$$

The second pattern (Cut II) is taken along the oblique cut which is a great circle orthogonal to the plane defined by (2.17) and is described by

$$\gamma = p\,5^o$$
$$\theta = \cos^{-1}(\cos\gamma\cos\theta_o) \qquad (2.18)$$
$$\phi = \phi_o+\sin^{-1}(\sin\gamma/\sin\theta) \quad .$$

When $\theta=0^o$ in Cut II, it is necessary to specify that $\phi=\phi_o$. Both of these cuts pass through the center of the patterns (θ_o, ϕ_o).

Equation (2.15) and all its related conditions have been programmed for computer evaluation. The output of the program gives $A(\theta, \phi)$ real, $A(\theta, \phi)$ imaginary, $|A(\theta, \phi)|^2$ and $|A(\theta, \phi)|^2 / |A(\theta_o, \phi_o)|^2$ in db. It is important to arrange the program in an efficient manner because the time required to evaluate (2.15) could be prohibitively long. Currently, it takes about 8 seconds to compute $A(\theta, \phi)$ 72 times for one pattern over Cut I or Cut II.

2.3 Patterns with Phase Control

Figures 1 - 4 show the normalized patterns with phase control according to eq. (2.15). A hemisphere aperture distribution ($\Delta_{nm} > 0$) which has between 76 and 80 active elements was excited for the data in the first four figures. The small variation in the number of active elements is due to the slight change in element distribution seen from different positions (θ_o, ϕ_o).

A comparison between Cuts I and II is presented in Fig. 1 for the case $a/\lambda = 1.5$, $\theta_o=90^o$, and $\phi_o=0^o$. Here the polar cut follows a path along the meridian $\phi=\phi^o$ and the oblique cut follows a path along the equator, $\theta = 90^o$. The 3 db difference in the first sidelobe levels in the two patterns of Fig. 1 is unusually high compared to the cases

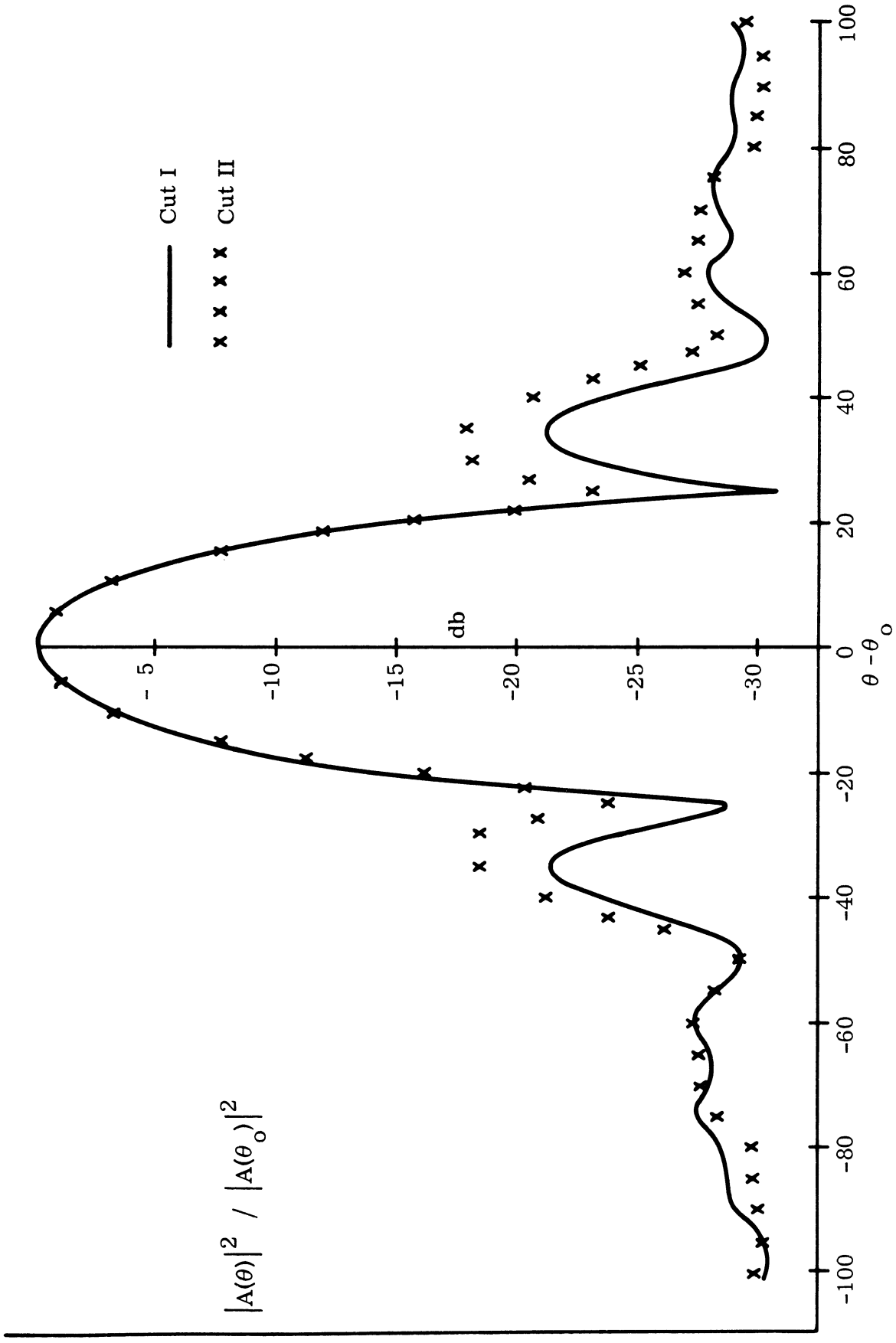

FIG. 1: RADIATION PATTERNS WITH PHASE CONTROL FOR CUTS I AND II WHEN $a/\lambda = 1.5$, $\theta_o = 90^o$ and $\phi_o = 0^o$.

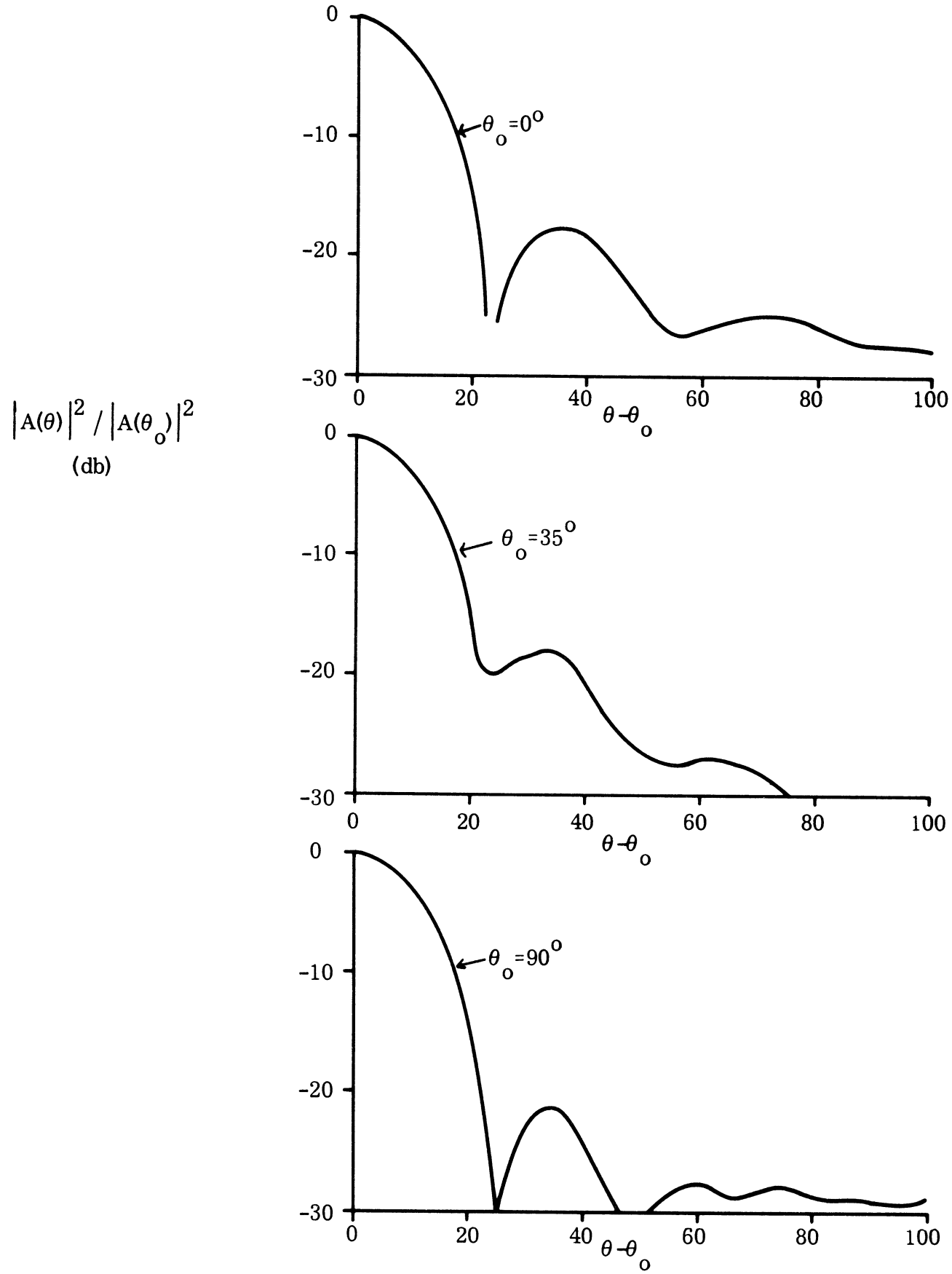

FIG. 2: Variation in Patterns with Phase Control for Beam Steering Over $\theta_o=0^o$, 35^o and 90^o (Cut I, $a/\lambda=1.5$, and $\phi_o=0^o$).

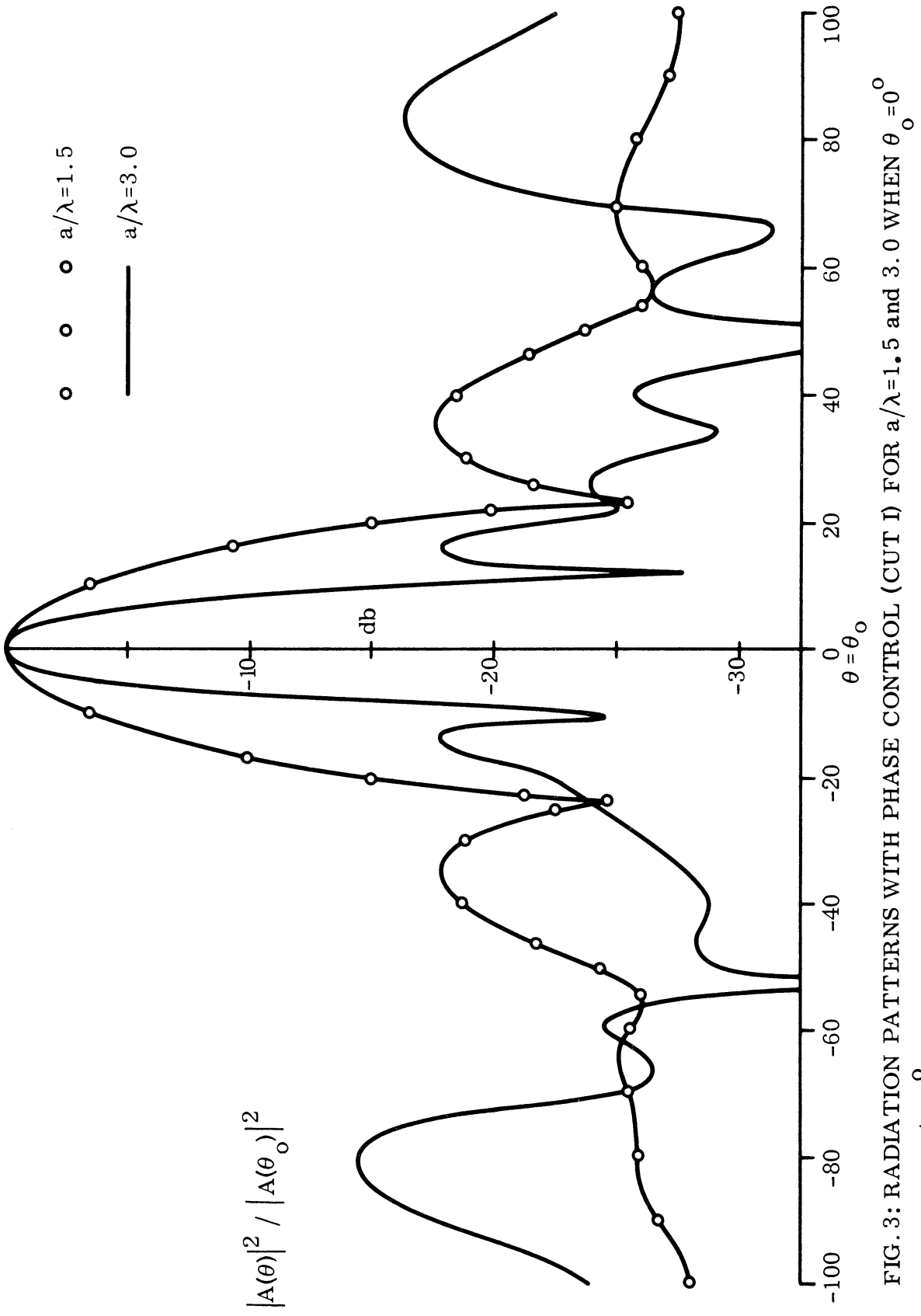

FIG. 3: RADIATION PATTERNS WITH PHASE CONTROL (CUT I) FOR $a/\lambda=1.5$ and 3.0 WHEN $\theta_o=0^o$ AND $\phi_o=0^o$.

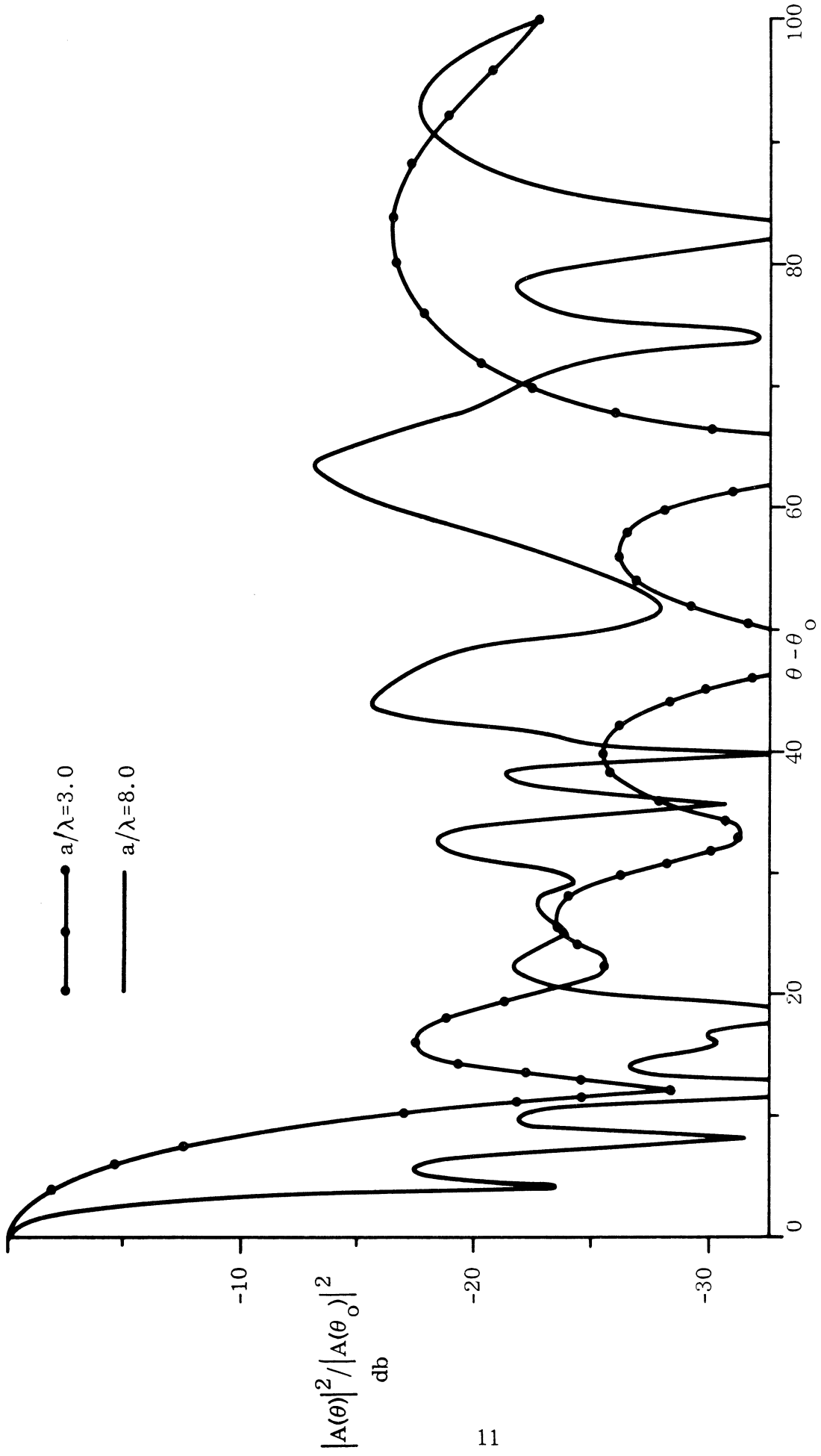

FIG. 4: RADIATION PATTERNS WITH PHASE CONTROL (CUT I) FOR $a/\lambda = 3.0$ and 8.0 WHEN $\theta_o = 0^o$ and $\phi_o = 0^o$.

when $\theta_o=0^o$ and $\theta_o=35^o$ (Fig. 2). This discrepancy is due to a difference in element distribution along the meridan and the equator. Steps are being taken to correct this variation in the element distribution.

There are minor changes in the patterns as the beam is steered over the hemisphere. Figure 2 shows three patterns for the polar cut when $\theta_o=0^o$, 35^o and 90^o while the rest of the parameters are held constant. The main beam is the same for the three patterns, but the first sidelobe for $\theta_o=90^o$ differs by 3 db from the other two cuts.

Figures 3 and 4 illustrate the effect of a/λ or ka on the radiation patterns for Cut I when $\theta_o=0^o$ and $\phi_o=0^o$. In Fig. 3, a/λ is 1.5 and 3.0 which correspond to 0.4λ and 0.8λ surface spacing between the elements respectively. A subsidiary lobe of amplitude -14db resembling a grating lobe appears near $\theta-\theta_o=90^o$ when $a/\lambda = 3.0$. More subsidiary lobes are present when $a/\lambda=8.0$ (2.13λ surface spacing) as seen in Fig. 4 where a/λ is 3.0 and 8.0.

After studying the computed patterns of the spherical array we conclude that typically the first sidelobe level is -18 db and the second is -24 db. For $a/\lambda > 3$ additional subsidiary lobes appear in the pattern.

2.4 Patterns without Phase Control

Figures 5, 6 and 7 show the patterns produced by the array when no systematic phasing is introduced into the individual antenna elements. This means that $\Delta_{nm}=\eta_{nm}=0$ in the exponent of eq. (2.15). However, the term Δ_{nm} is retained in (2.16) as the condition governing the aperture position and size or the number of activated elements. The parameters θ_o, ϕ_o in this case specify the axis of symmetry of the activated aperture. The following table gives the number of active elements as Δ_{nm} is varied.

$\Delta_{nm}(\theta_o=0^o, \phi_o=0^o)$	No. of Active Element
> 0	76
> 0.70	26
> 0.86	16

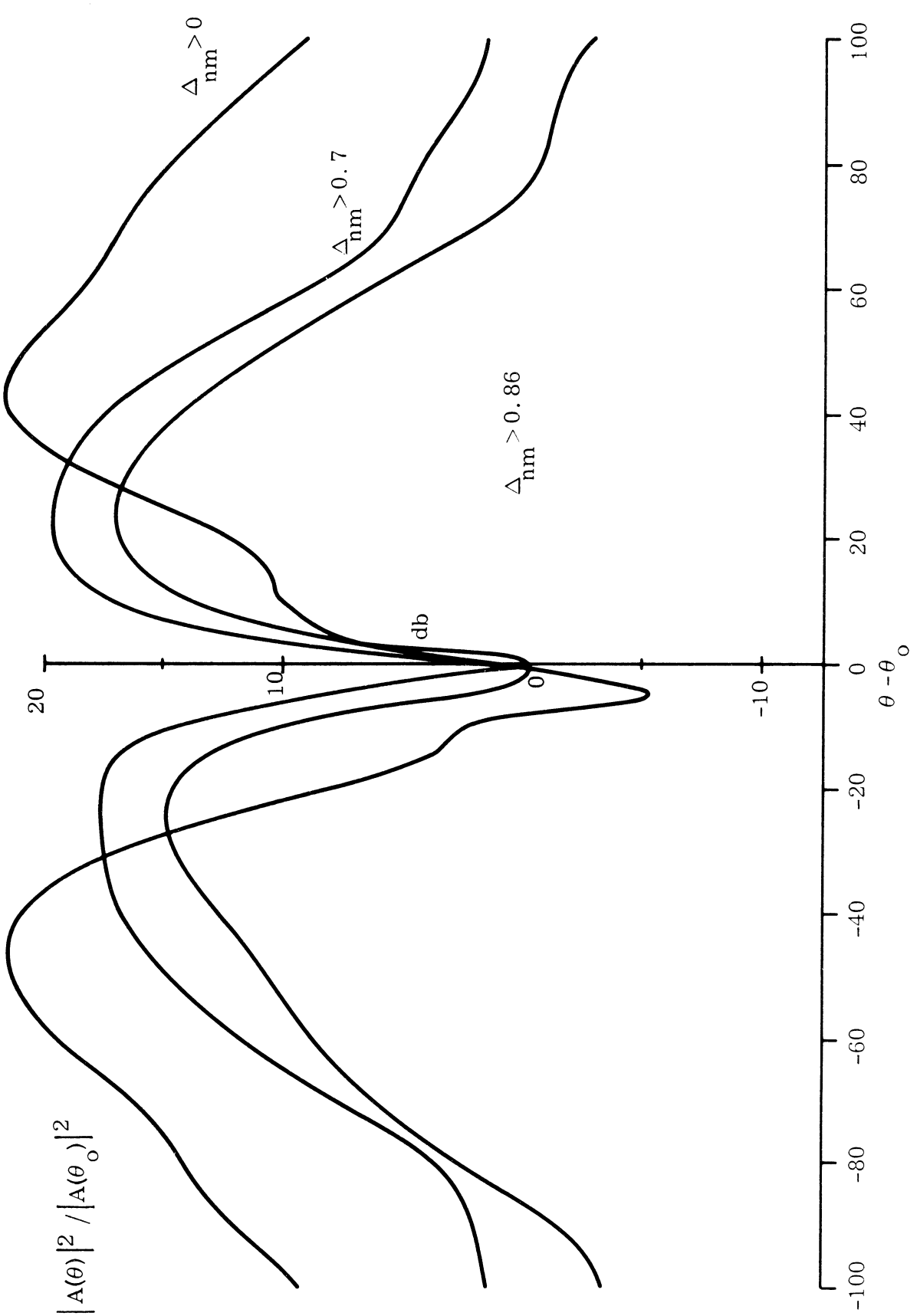

FIG. 5: RADIATION PATTERNS WITHOUT PHASE CONTROL FOR APERTURE VARIATIONS $\Delta_{nm}>0$, $\Delta_{nm}>0.7$ and $\Delta_{nm}>0.86$ (CUT I, $a/\lambda=1.5$, $\theta_o=0^o$ and $\phi_o=0^o$).

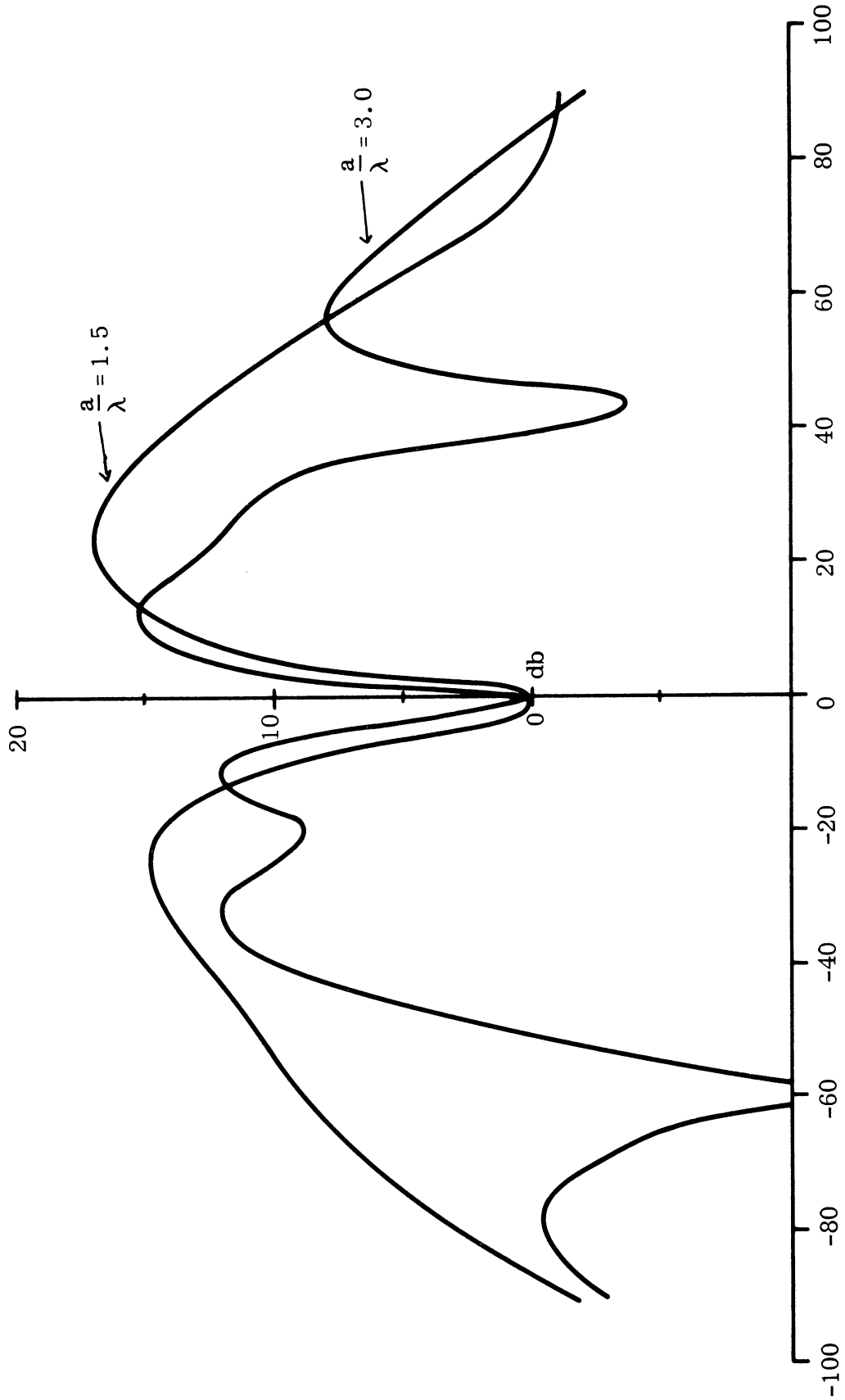

FIG. 6: RADIATION PATTERNS WITHOUT PHASE CONTROL FOR $a/\lambda = 1.5$ and 3.0
(CUT I, $\theta_o = 0^o$, $\phi_o = 0^o$ AND $\Delta_{nm} > 0.86$).

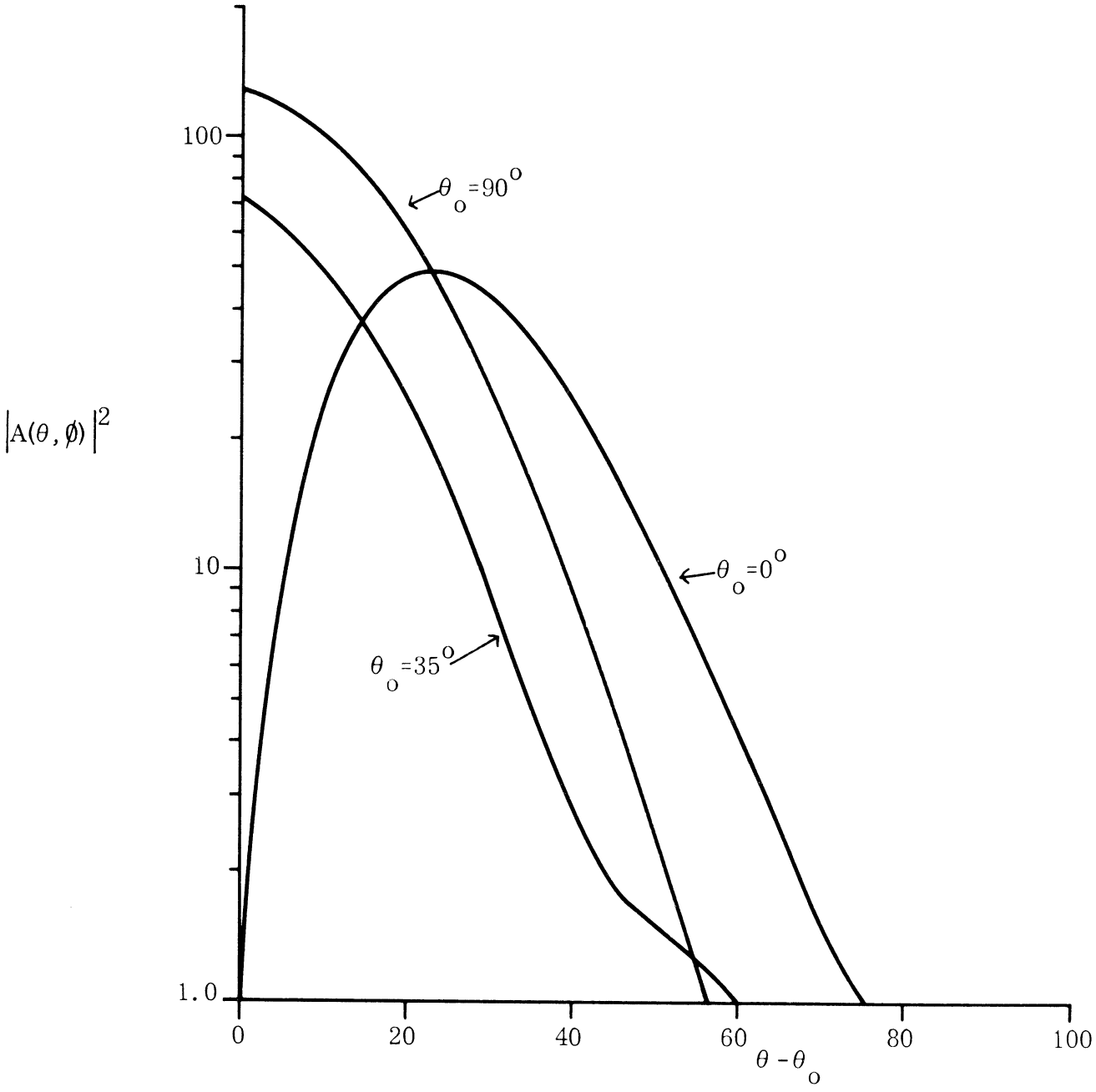

FIG. 7: VARIATIONS IN PATTERNS WITHOUT PHASE CONTROL FOR BEAM STEERING OVER $\theta_o=0^o$, 35^o and 90^o (CUT I, $a/\lambda=1.5$, $\phi_o=0^o$ AND $\Delta_{nm}=0.86)^o$.

It can be seen from Figs. 5 and 6 that when $\theta=\theta_0=0^o$ a sharp minimum occurs at the position $\theta-\theta_0=0^o$ of the patterns. This is in contrast to the case with phase control when there is a maximum along $\theta-\theta_0=0^o$. The position of the minimum is found to be independent of a/λ but it is dependent on the section of the sphere which is activated. This can be seen from Fig. 7 which shows the patterns in arbitrary scale when different portions of the sphere are activated. This suggests that by rearranging the angular position of each element about its own axis, it may be possible to produce patterns which become less dependent on the position of the activated area. This needs more investigation.

2.5 Directivity

According to Kraus (1950) the directivity D of an antenna is defined as

$$D = \frac{4\pi\, A_{max}(\theta,\phi)^2}{\int_0^{2\pi}\int_0^{\pi} |A(\theta,\phi)|^2 \sin\theta\, d\theta\, d\phi} \quad . \tag{2.19}$$

The array factor $A(\theta,\phi)$ in this case is too complicated to integrate, so the following approximation is made.

$$D = \frac{2\left|A_{max}(\theta)\right|^2}{\Delta\theta \sum_{0^o}^{180^o} |A(\theta)|^2 \sin\theta} \tag{2.20}$$

where it has been assumed that $A(\theta)$ is symmetric with respect to ϕ. The constant increment $\Delta\theta$ must be chosen smaller than the angular width of major pattern fluctuations.

If most of the power is in the main lobe of the pattern, a simpler expression for directivity is

$$D = 41,253/\theta_B\phi_B \tag{2.21}$$

where θ_B and ϕ_B are the half-power beam widths of the two cuts measured in degrees.

Directivity calculations have been made for the two patterns in Fig. 3. For the case $a/\lambda=1.5$, D = 19.13 db according to eq. (2.20) and 20 db according to (2.21). For the pattern with $a/\lambda=3.0$, D=20.5 db by (2.20) and 26 db by (2.21) . Due to the subsidiary lobe in the case of $a/\lambda=3$ the simplified expression in (2.21) is not valid. It is also noticed that the width of the subsidiary lobe is broader than the main beam. This can be explained by the fact that the aperture has decreased in size because part of it is no longer visible at $\theta-\theta_0$ near 90^o.

III

SUBSIDIARY LOBES IN THE PATTERNS OF NONPLANAR ARRAYS

In Section 2.3 it has been found that large subsidiary lobes resembling the grating lobes in the case of uniform planar or linear arrays appear in the patterns of the spherical array for wide spacing between the elements. The behavior of these large amplitude lobes is different than those in the planar uniform arrays. In this Chapter we report on the results of a study of the space factor of a circular array of isotropic elements when the spacing between the adjacent elements is of the order of or larger than a wavelength. Although the particular case discussed below is idealized, it is hoped that the results of the investigation will be useful in understanding the case when the elements are widely spaced on a curved surface.

3.1 Circular Array Pattern

During the past few years many papers have been published on the patterns produced by circular arrays of isotropic elements (Knudsen 1956; Neff and Tillman 1960). However all of them were concerned with the case when the spacing between the adjacent elements is less than $\lambda/2$ or in other words, for a given diameter of the array, the number of elements is chosen to be sufficiently large so as to satisfy this condition. This condition amounts to replacing the array of discrete elements by a continuous current ring of appropriate phase whose pattern does not have any grating lobe. The above approximation breaks down in cases when the element spacing is of the order of or larger than $\lambda/2$. In the following sections we investigate the pattern under these circumstances. Only the pertinent results are reported here; the details of the analysis may be found in Sengupta (1966).

The array is assumed to consist of isotropic elements, placed uniformly along the circumference of a circle. The elements are excited with equal amplitudes but their relative phases are so adjusted that the resulting pattern has a maximum along a certain direction. Let us assume that the number of elements used is M and the radius of the circular array is a. The plane of the array is in the xy-plane of a

Cartesian coordinate system xyz with the origin at the center of the circle which is also taken to be the phase center of the array. It can be shown that the pattern produced by such an array is given by

$$A(\theta,\phi)=J_0(r)+2\sum_{n=1}^{\infty} J_{Mn}(r)\cos\left[Mn\left(\frac{\pi}{2}-\xi\right)\right] \quad \text{, if M is even ,} \tag{3.1}$$

$$A(\theta,\phi)=J_0(r)+2\sum_{n=1}^{\infty} J_{2Mn}(r)\cos\left[2Mn\left(\frac{\pi}{2}-\xi\right)\right]$$

$$+2i\sum_{n=0}^{\infty} J_{M(2n+1)}(r)\cos\left[M(2n+1)\left(\frac{\pi}{2}-\xi\right)\right], \quad \text{if M is odd,} \tag{3.2}$$

where

J_{Mn} is the Bessel function of the first kind and order Mn,

$$r^2=(ka)^2\left[\sin^2\theta+\sin^2\theta_0-2\sin\theta\sin\theta_0\cos(\phi-\phi_0)\right] , \tag{3.3}$$

$$\tan\xi=\left[\frac{\sin\theta\sin\phi-\sin\theta_0\sin\phi_0}{\sin\theta\cos\phi-\sin\theta_0\cos\phi_0}\right] , \tag{3.4}$$

θ_0, ϕ_0 specify the position of the maximum in the pattern.

If M is sufficiently large, both (3.1) and (3.2) may be well approximated by the first term $J_0(r)$ only; the rest of the terms are referred to as the correction terms and are usually negligible if M is very large. Note that the spacing in wavelengths between the adjacent elements is given by $s_\lambda = ka/M$. When the element spacing is comparable to or larger than a wavelength the effects of the correction terms in (3.1) and (3.2) cannot be neglected.

If $\theta_o=\pi/2$ and $\theta=\pi/2$, i. e. we wish to find the pattern in the plane of the array, then it can be shown that (3. 1) and (3. 2) reduce to

$$A(\phi)=J_0(2ka\sin\frac{\phi-\phi_o}{2})+2\sum_{n=1}^{\infty}J_{Mn}(2ka\sin\frac{\phi-\phi_o}{2})\cos\left[Mn\frac{\phi+\phi_o}{2}\right], \qquad (3.5)$$

when M is even,

and

$$A(\phi)=J_0(2ka\sin\frac{\phi-\phi_o}{2})+2\sum_{n=1}^{\infty}J_{2Mn}(2ka\sin\frac{\phi-\phi_o}{2})\cos\left[Mn(\phi+\phi_o)\right]$$

$$-2i\sum_{n=0}^{\infty}J_{M(2n+1)}(2ka\sin\frac{\phi-\phi_o}{2})\sin\left[M(2n+1)(\frac{\phi+\phi_o}{2})\right],$$

when M is odd . (3. 6)

It should be mentioned that the exact pattern in this case for both M even and odd is given by

$$A(\phi)=\sum_{m=1}^{M}e^{ika\left\{\cos(\frac{2\pi}{M}m-\phi)-\cos(\frac{2\pi}{M}m-\phi_o)\right\}} . \qquad (3.7)$$

Analytically one can obtain more information about the pattern from eqs (3. 5) and (3. 6) than from (3. 7). In the next section we study eq. (3. 5) in greater detail.

3. 2 Pattern in the Array Plane : M even

Consider the case when $\phi_o=0$. Thus we obtain the following from (3. 5)

$$A(\phi)=J_0(2ka\sin\frac{\phi}{2})+2\sum_{n=1}^{\infty}J_{Mn}(2ka\sin\frac{\phi}{2})\cos\frac{Mn\phi}{2} . \qquad (3.8)$$

If $M\gg 2ka$ then the pattern can be approximated as follows

$$A(\phi)\approx J_0(2ka\sin\frac{\phi}{2}) . \qquad (3.9)$$

In this case the sidelobes in the pattern correspond to the secondary maxima of the zeroth order Bessel function in (3.9). The table below gives the positions and levels of the first few sidelobes compared to the main beam at $\phi=0$.

Position ($2ka \sin \phi/2$)	Sidelobe Level (db)
3.8	- 7.90
7.0	-10.45
10.2	-12.05
13.3	-13.22

The half-power beamwidth defined as the angle between the two half-power points of the pattern as predicted by (3.9) is

$$2\phi_{1/2} = 4 \sin^{-1} \left(\frac{1.13}{2ka}\right) \quad . \tag{3.10}$$

It can be shown that the beamwidth is given by the same expression (3.10) when the beam maximum is adjusted to be along the direction $\phi=\phi_0$. One finds in this case the beamwidth is independent of the steering angle ϕ_0.

Figure 8 shows the exact pattern calculated by using (3.7) with $\phi_0=0$, M=8 and $ka=\pi$ (i.e. $a=\lambda/2$). The spacing between the elements is $s_\lambda=0.3925$. The approximate pattern calculated from (3.9) is also shown in Fig. 8. The agreement between the two is very good except for values of ϕ near π. For the same values of ka if M is made larger, the approximation should be better. Thus it may be concluded that if $s_\lambda \ll 1/2$ the pattern will not have any maxima other than those predicted by the zeroth order Bessel function in (3.9).

3.3 Pattern for Large Spacing

Figure 9 shows the exact pattern with $\theta_0=\pi/2$, $\phi_0=0$, M=8 and $ka=2\pi(a=\lambda)$. In this case the spacing between the adjacent elements is $s_\lambda = 0.785$ and $M < 2ka$. As compared to Fig. 8 ($s_\lambda < 1/2$) the pattern in this case develops some large subsidiary maximum. The zeroth order term can only explain fairly well the main beam and the first sidelobe but it becomes a very poor approximation beyond the first sidelobe. The pattern calculated by taking the first two terms in (3.8) is

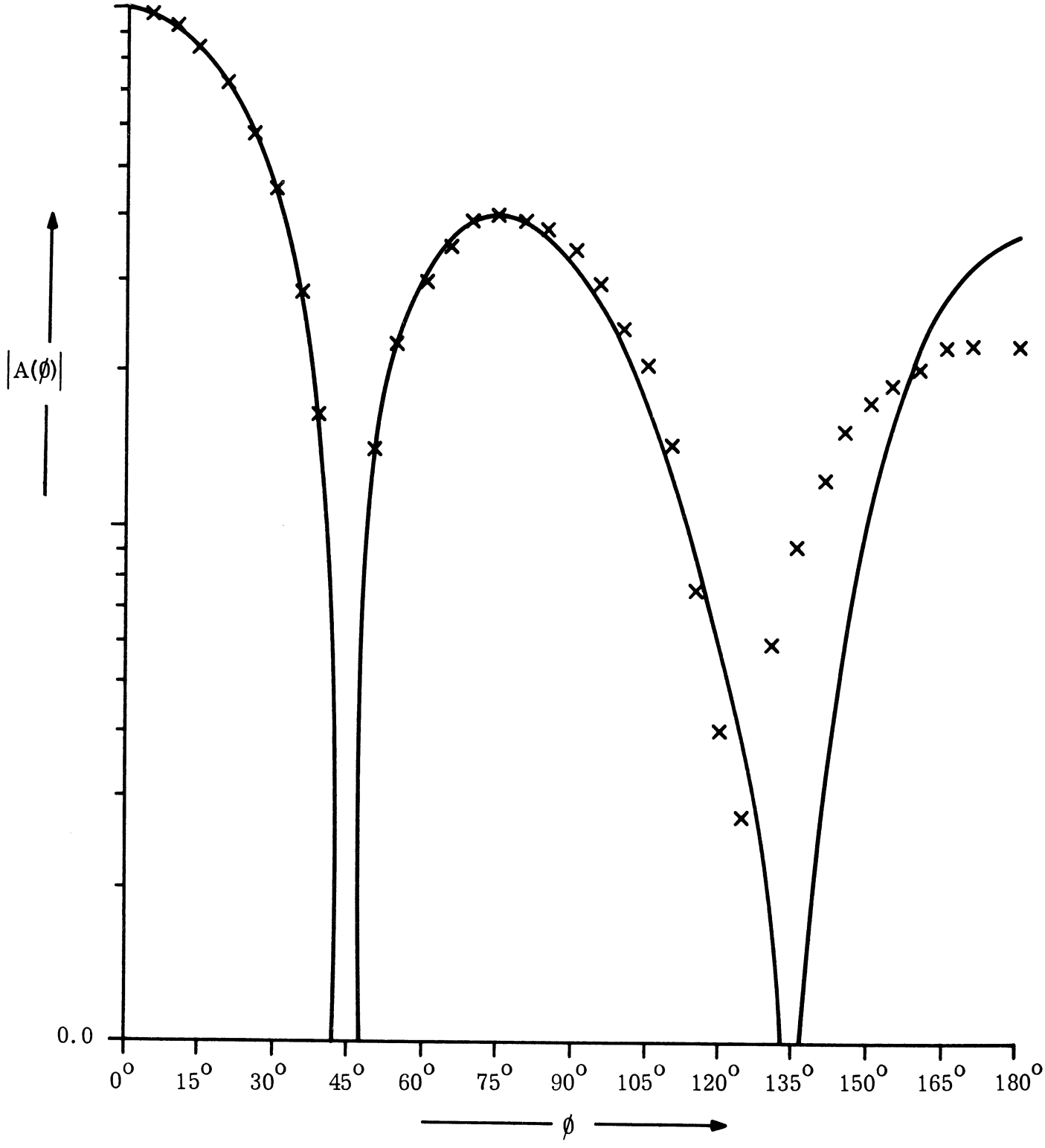

FIG. 8: THE RADIATION PATTERN PRODUCED BY A CIRCULAR ARRAY.
M=8, a=λ/2 (——) exact pattern (xxx) approximate pattern

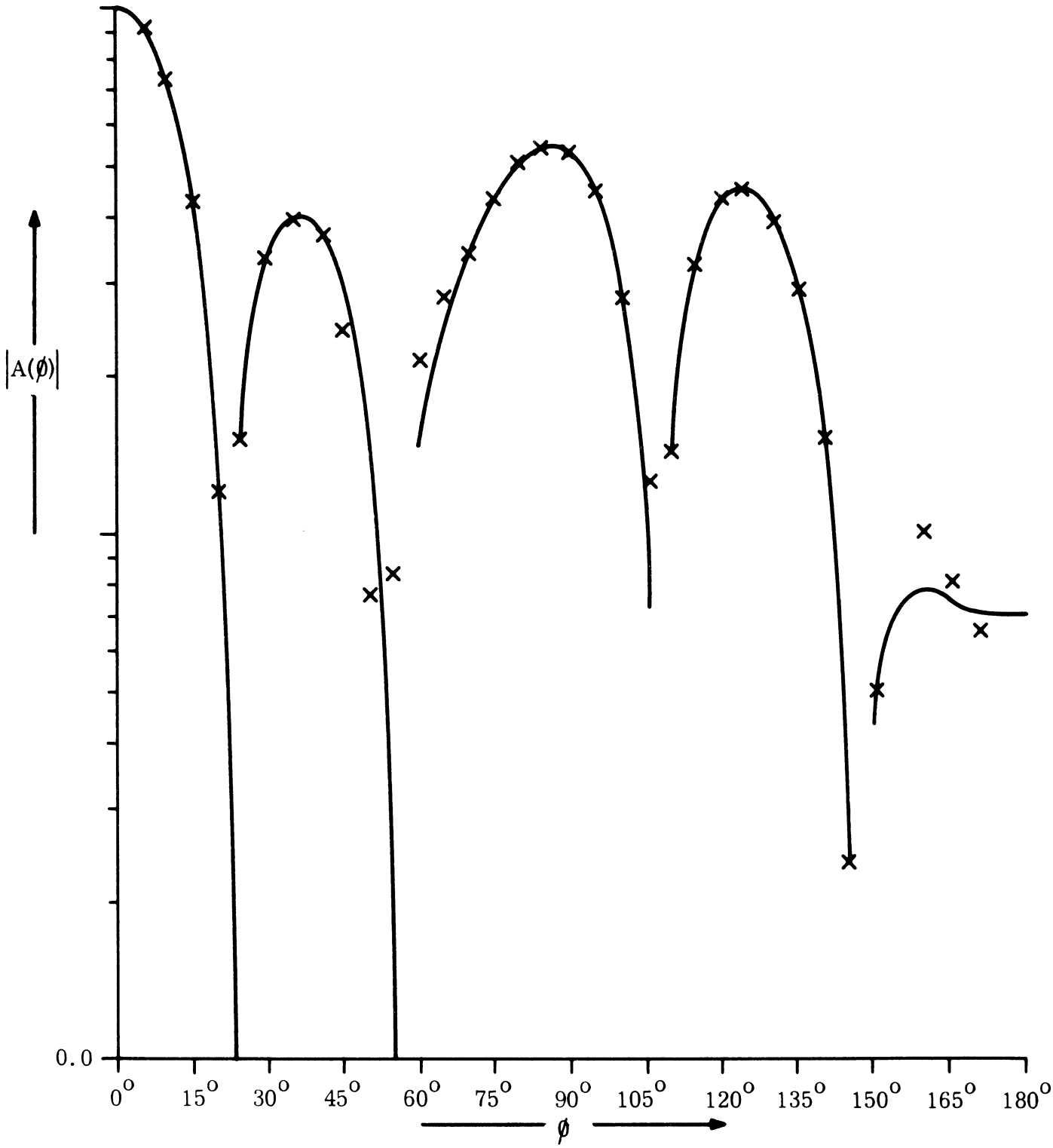

FIG. 9: THE RADIATION PATTERN PRODUCED BY A CIRCULAR ARRAY.
M=8, a=λ (——)exact pattern, (x x x) approximate pattern.

also superposed on Fig. 9. The agreement between the two is found to be good. The rest of the terms in eq. (3.8) contribute very little because of the fact that for all those terms the arguments of the Bessel functions are progressively smaller than the orders. Hence, for constant M as 'ka' is made larger, more and more terms will be needed for better approximation. This suggests that by studying the variation of the first few terms the locations and the amplitudes of the dominant subsidiary lobes may abe approximately predicted.

The correction terms in (3.8) take on large values whenever the argument $(2ka \sin \frac{\phi}{2})$ takes on values comparable to Mn. We may then expect to have subsidiary maxima in the pattern in the region of ϕ where one of the correction terms become large. With large M and ka one needs tables of higher order Bessel functions which are not readily available. We need to investigate the functions particularly in the region where both the order and argument are large and nearly equal. In this region we can make use of the Fock approximation to Bessel function developed in diffraction theory (Logan, 1957). For large order and argument we can write

$$J_{Mn}(2ka \sin \frac{\phi}{2}) \approx \frac{Ai(t)}{(\frac{\rho}{2})^{1/3}}, \tag{3.11}$$

where

$$\rho = 2ka \sin \frac{\phi}{2} \tag{3.12}$$

$$t = \frac{Mn-\rho}{(\frac{\rho}{2})^{1/3}}$$

and Ai(t) is the Airy function defined as

$$Ai(t) = \frac{1}{\pi} \int_0^\infty \cos\left(\frac{x^3}{3} + tx\right) dx \quad . \tag{3.14}$$

Tables of Airy functions are available in the literature. Thus, in the neighborhood of a subsidiary maxima the pattern can be presented as

$$A(\phi) \quad J_o(2ka \sin \frac{\phi}{2}) + 2 \sum_{n=1}^{\infty} \frac{Ai(t)}{(\frac{\rho}{2})^{1/3}} \cos \frac{Mn\phi}{2} \quad . \tag{3.15}$$

Equation (3.15) is a highly convergent series. The first two maxima of Ai(t) are given by

$$\left.\begin{aligned} Ai(t_1) &= +0.5356 \qquad & t_1 &\doteq -1.02 \\ Ai(t_2) &= -0.4174 \qquad & t_2 &\doteq -3.25 \end{aligned}\right\} \quad . \tag{3.16}$$

Using the values of t_1 or t_2, we can solve (3.13) for values of ρ where there may be a subsidiary maximum. Taking $t_1 = -1.02$, the required ρ will be obtained from the real root of the following cubic equation

$$y^3 - 3py - 2q = 0 \quad , \tag{3.17}$$

where

$$p = \frac{1.02}{2^{1/3} \cdot 3} \quad , \qquad q = Mn/2 \quad , \tag{3.18}$$

$$\rho = y^3 \quad . \tag{3.19}$$

The real root of (3.17) is

$$y = 2\sqrt{p} \cosh \frac{\eta}{3} \quad , \qquad \cosh \eta = \frac{q}{\sqrt{p^3}} \quad . \tag{3.20}$$

For each value of n, ρ will be different, thus we may account for the positions of the various subsidiary lobes by using (3.12). If for some value of n, eq. (3.12) predicts a complex value of ϕ, then we should solve (3.17) for ρ with $p = 3.25/2^{1/3} \cdot 3$ (i.e. $t_2 = -3.25$) and thereby obtain the position of the maximum. Once the location of the maximum is determined we obtain the approximate maximum value of $A(\phi)$ by summing the first two or three terms. The positions and levels of the subsidiary maxima as calculated in the above manner are shown in the following table for the case when $ka = 4\pi$, $M=8$.

Subsidiary Max.	Approximate Position	Amp.	Exact Position	Amp.
1	$45^{o}48'$	0.861	46^{o}	0.863
2	$92^{o}56'$	0.891	92^{o}	0.881
3	-	-	136^{o}	0.862

Figure 10 shows the exact pattern produced for the case M=8, $ka=4\pi$ ($a=2\lambda$). In this case the spacing between the elements is $s_\lambda=1.57$. Here the subsidiary lobes are almost equi-amplitude and are quite large in value.

3.4 Discussion

In the above we have discussed the pattern produced by a circular array of even number isotropic elements when the element spacing is comparable to wavelength. From the analysis and study of a few exact patterns computed, we make the following comments.

3.4.1.

For element spacing $s_\lambda < 1/2$ the space factor may be approximated by the zeroth order Bessel function of proper argument. In this case the pattern is determined by the radius of the array only and is independent of the number of elements M, as long as M is large. The half-power beamwidth of the pattern is independent of the beam steering angle ϕ_o. This is in contrast to the uniform planar case where the beam deteriorates with more and more steering.

3.4.2.

Subsidiary lobes resembling the grating lobes appear in the pattern when $s_\lambda > 1/2$. These lobes grow in amplitude as s is increased by keeping M constant. We have calculated the pattern for various values of ka with M=8. As ka is increased more and more subsidiary lobes appear in the pattern but their amplitudes at first grow, and than again fall down for larger values of s_λ. There appears to be some particular value of s_λ for a given M where the subsidiary maxima take on their largest value. This needs more investigation. There is no case, however, where the subsidiary maxima is as large as the main beam.

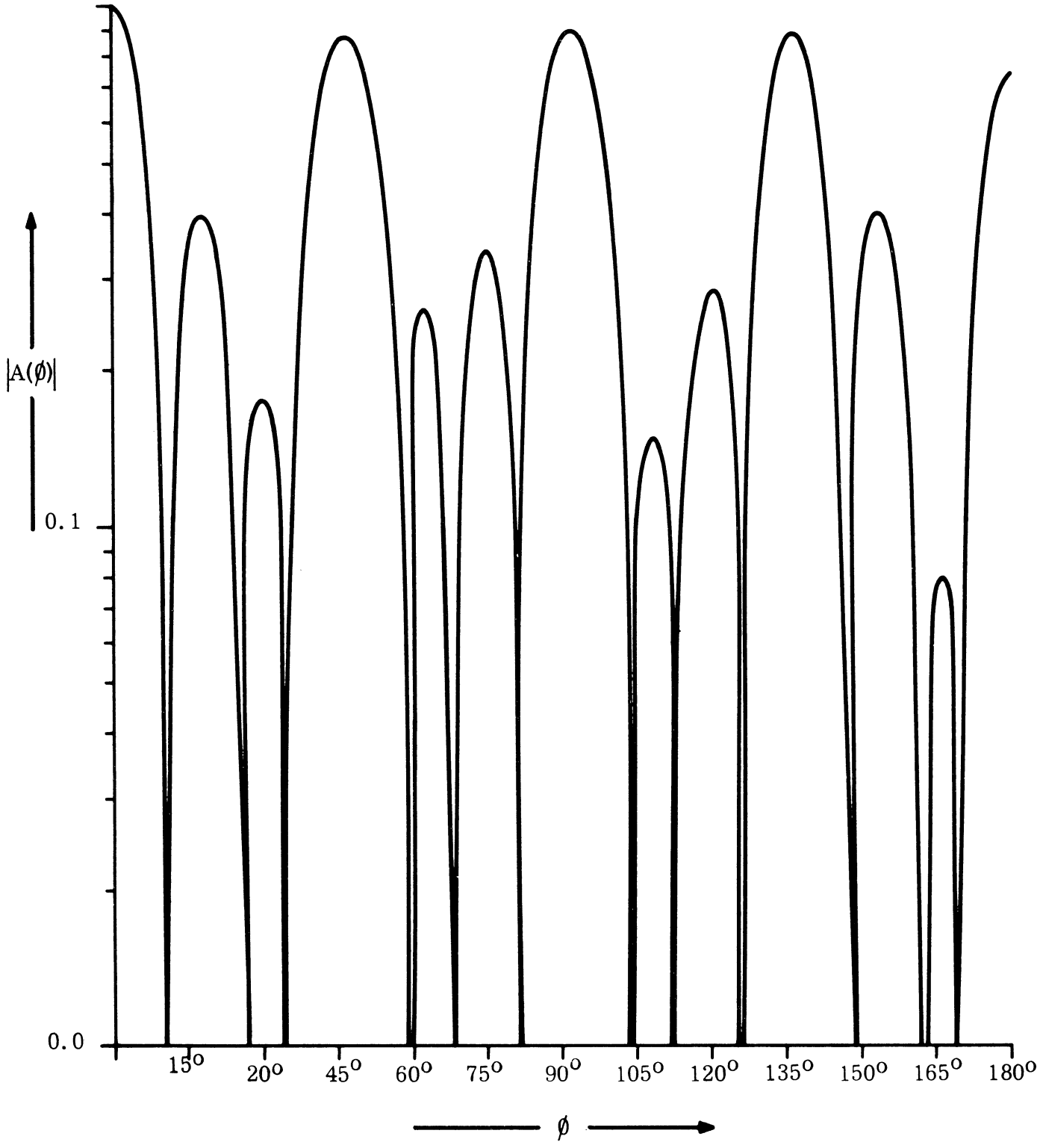

FIG. 10: RADIATION PATTERN OF A CIRCULAR ARRAY. $M = 8$, $a = 2\lambda$.

3.4.3.

For the same value of s_λ if M is increased the maxima of the subsidiary lobes are decreased. This is because the first maximum value of $J_M(\rho)$ decrease with increasing M (c.f. eq. (3.8)).

3.4.4.

We have discussed the pattern produced in the plane of a circular array of isotropic elements. Only the case of even number of elements has been discussed. From eq. (3.3) one may expect the pattern to be better when M is odd. This will be investigated in the future.

For spacing between the elements of the order of or greater than $\lambda/2$ there appear subsidiary maxima in the pattern resembling the familiar grating lobes in the uniform planar arrays with large element spacing. However, the behavior of these subsidiary lobes are different from the latter case. We have developed an approximate procedure to predict subsidiary maxima and plan to investigate this method further.

IV
CORRELATION PROCESSING OF THE OUTPUT DATA

The bulk and inertia of microwave and VHF phase shifters have stimulated an investigation of a signal processing method which does not require individual variable phase delay for each antenna element. In this chapter we shall describe briefly a system which eliminates the phase shifters at the cost of a certain loss in signal-to-noise ratio.

It is customary to specify the directional properties of an antenna array by its 'radiation pattern' obtained by calculating the field intensity produced at a distant point by the sum of the contributions from all the antenna elements. By reciprocity this pattern also specifies the performance of the array for receiving purposes. However, for the present analysis it is preferable to derive the array properties from its response to an incident plane wave.

If the antenna elements are distributed over a conducting spherical surface, the direction-finding problem involves three different steps:

1) Solution of the boundary-value problem of a plane wave incident on a conducting sphere for all desired angles of incidence, frequencies and polarizations.

2) Sampling of the field along the spherical surface by a finite number of antenna elements.

3) Processing the output from all the elements in order to obtain the angle of incidence and general performance characteristics, such as resolution, antenna pattern, etc.

We are concerned here with the third item, the first operation of which can be described as calculating from the array signals an approximate value of the correlation between the unknown incident signal and a standard signal of known angle of incidence and the same frequency as the incident signal. The square of this approximate correlation is identical to the corresponding value of the conventional radiation pattern of the array.

The data for the standard waves are permanent parts of the program or memory of the signal processing equipment.

In order to present the principle of the correlation processing as simply and clearly as possible, we shall consider scalar waves and isotropic antenna elements only, i. e. disregarding individual element patterns and polarization effects. An extension to a more general and realistic treatment is straightforward and is strictly analogous to the analysis presented in the first quarterly report (Sengupta et al, 1965).

4. 1 Correlation Analysis of the Output Data

Let a_{ij} be the matrix of elements distributed over the array surface and $\chi_{ij}(t)$ the output voltage of each element, which is assumed to be approximately monochromatic, i. e.

$$\chi_{ij}(t) = Z_{ij}\cos(\omega t + \phi_{ij}) \tag{4.1}$$

where Z_{ij} is a constant or a slowly varying function of time. This output voltage $\chi_{ij}(t)$ is correlated with two unit voltages 90^{o} out of phase but having the same frequency as the incident wave. The resulting correlation components

$$X_{ij} = \frac{1}{T}\int_{T} \chi_{ij}(t)\cos\omega t\, dt \qquad (T \gg 2\pi/\omega) \tag{4.2}$$

$$Y_{ij} = \frac{1}{T}\int_{T} \chi_{ij}(t)\sin\omega t\, dt \tag{4.3}$$

contain all the amplitude and phase information about the incident wave. This general approach was already implied by Woodward (1953) and has more recently been suggested by Kendall (1963).

Now let

$$s_{ij}(t) = S_{ij}\cos(\omega t + \theta_{ij} + \theta_{o}) \tag{4.4}$$

be the signals produced by a wave of known angle of incidence and known amplitude. Then, also the 'weighting factors'

$$P_{ij} = \frac{1}{T}\int_{T} s_{ij}(t)\cos\omega t\, dt \tag{4.5}$$

$$Q_{ij} = \frac{1}{T}\int_T s_{ij}(t)\sin\omega t\, dt \tag{4.6}$$

are known functions of the angle of incidence.

The correlation between the incident wave and the reference wave is then proportional to

$$R = \sum_{i,j} \frac{1}{T}\int_T \chi_{ij}(t)s_{ij}(t)\, dt \quad . \tag{4.7}$$

Because of the unknown phase difference θ_o between the two waves, we need also a 'conjugate' correlation

$$\bar{R} = \sum_{i,j} \frac{1}{T}\int_T \chi_{ij}(t)s_{ij}(\tau+\frac{\pi}{2\omega})dt \tag{4.8}$$

Considering Z_{ij} and S_{ij} as time invariants we obtain the following relations

$$X_{ij} = \frac{1}{2} Z_{ij}\cos\phi_{ij} \tag{4.9}$$

$$Y_{ij} = -\frac{1}{2} Z_{ij}\sin\phi_{ij} \tag{4.10}$$

$$P_{ij} = \frac{1}{2}S_{ij}\cos(\theta_{ij}+\theta_o) = -\frac{1}{2} S_{ij}\sin(\theta_{ij}+\theta_o+\frac{\pi}{2}) \tag{4.11}$$

$$Q_{ij} = -\frac{1}{2} S_{ij}\sin(\theta_{ij}+\theta_o) = -\frac{1}{2} S_{ij}\cos(\theta_{ij}+\theta_o+\frac{\pi}{2}) \tag{4.12}$$

$$R = \sum_{ij} 2\left[X_{ij}P_{ij}+Y_{ij}Q_{ij}\right] \tag{4.13}$$

$$\bar{R} = \sum_{ij} 2\left[X_{ij}Q_{ij}-Y_{ij}P_{ij}\right] . \tag{4.14}$$

In order to remove the dependence on θ_o the following alternate expressions may be derived.

$$R=\cos\theta_o \sum_{ij} \frac{1}{2} Z_{ij}S_{ij}\cos(\phi_{ij}-\theta_{ij})+\sin\theta_o \sum_{ij} \frac{1}{2} Z_{ij}S_{ij}\sin(\phi_{ij}-\theta_{ij})$$

$$=A\cos\theta_o+B\sin\theta_o=\rho\sin\psi \qquad (4.15)$$

$$\bar{R}=\cos\theta_o \sum_{ij} \frac{1}{2} Z_{ij}S_{ij}\sin(\phi_{ij}-\theta_{ij})-\sin\theta_o \sum_{ij} \frac{1}{2} Z_{ij}S_{ij}\cos(\phi_{ij}-\theta_{ij})$$

$$=B\cos\theta_o-A\sin\theta_o=\rho\cos\psi \quad . \qquad (4.16)$$

Except for a normalizing factor, the amplitude of the correlation coefficient of the two waves consequently is

$$\rho=\left[R^2+\bar{R}^2\right]^{1/2}=\left[A^2+B^2\right]^{1/2}=2\left\{\sum_{ij}^{2}\left[X_{ij}P_{ij}+Y_{ij}Q_{ij}\right]+\sum_{ij}^{2}\left[X_{ij}Q_{ij}-Y_{ij}P_{ij}\right]\right\}^{1/2}, \qquad (4.17)$$

and its phase is

$$\psi=\theta_o+\tan^{-1}\frac{A}{B}=\tan^{-1}\frac{R}{R} \quad . \qquad (4.18)$$

The quantities R and $\bar{R}$ are simply weighted sums of the data X_{ij} and Y_{ij}. The weight factors P_{ij} and Q_{ij} provide the means for scanning.

Complete sequential search of the whole hemisphere is accomplished by an appropriate program of $P_{ij}(t)$ and $Q_{ij}(t)$. The maxima in ρ or ρ^2 observed during scanning indicate the peaks of the main lobe or side lobes of incident signals.

Equations (4.17) and (4.18) represent a transformation back from Cartesian to polar variables; the radius vector ρ represents the correlation that would have been obtained if the phase discrepancy θ_o were made equal to zero.

It is important to note that ρ is independent of the phase difference θ_o. As long as all data are processed simultaneously, a small frequency difference or phase slip can be tolerated. The reciprocal of this frequency difference should be large in comparison with the integration time T. The square of ρ plotted versus scanning angle traces exactly the conventional radiation pattern of the antenna array, except for a scale factor.

Figure 11 shows a block schematic of a correlation system for direction finding. A certain amount of errors in the radio-frequency circuits can easily be compensated for if the weight factors P and Q are determined by calibration rather than by theoretical computation.

4.2 Discussion

The advantages of this signal-processing procedure are:

1) A minimum of rf plumbing. No rf phase shifters are required. All phase adjustments are performed by means of the (Cartesian) weight factors P and Q.

2) all-electronic scanning is obtained by varying P and Q by electronic means (analog or digital computer). Since a number of correlators may operate in parallel, more than one 'scanning spot' may be operating independently at the same time. The scanning speed depends (at each frequency) primarily on the integration time in eqs. (4.2) and (4.3).

It appears advisable to perform the first correlation (4.2) and (4.3) at intermediate frequency so that the two reference voltages with 90^{o} phase difference have a fixed frequency.

The primary disadvantage of this system is that each and every antenna element requires a certain amount of equipment, converter, correlator and possibly amplifiers. This affects not only the cost and complexity but also the overall noise level of the system, since independent noise sourced are introduced into each element channel. However, a competitive system based on wide-band variable phase shifters is not without reflections and other channel losses which reduce the signal-to-noise ratio. In addition, the individual channel control equipment increases cost and complexity.

Some quantitative or semi-quantitative conclusions regarding the signal-to-noise ratio at the output of an antenna array can easily be formulated in terms of the antenna gain. If the main-lobe signal-to-noise ratio at the output of the system were predominantly determined by a uniform 'sky noise' of distant origin, the signal-to-noise improvement over an isotropic antenna would be equal to the antenna gain.

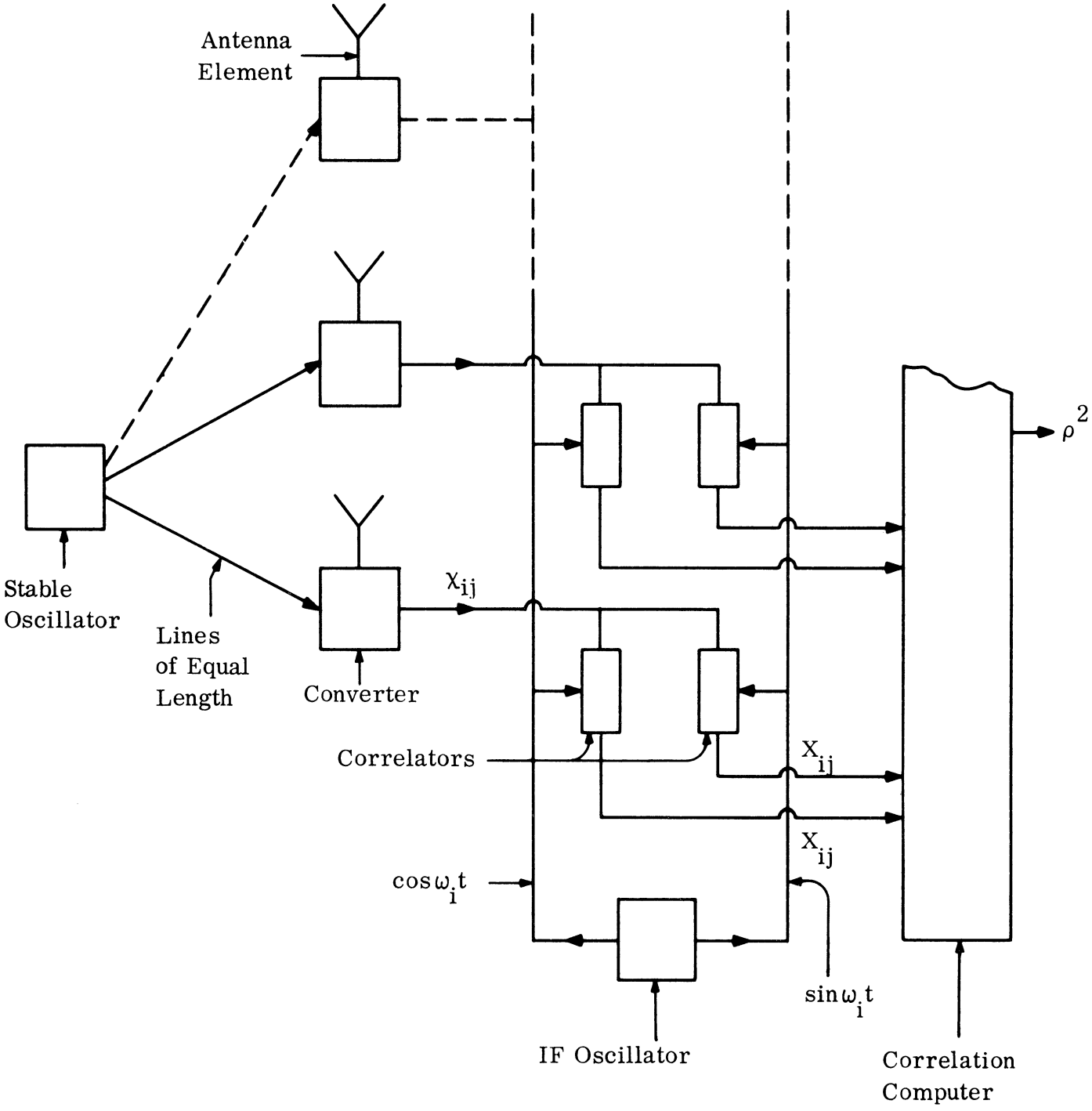

FIG. 11: BLOCK SCHEMATIC OF ARRAY WITH CORRELATION PROCESSING

On the other hand, if the signal-to-noise ratio were limited by the noise generated in the first electronic components in each channel, an improvement of the square root of the antenna gain could be expected, since in the main lobe the signal contributions add coherently while the independent noise powers add noncoherently.

An ideal phase-shifting array with all the electronic components in a single common channel would theoretically realize an improvement equal to the antenna gain also when the receiver noise predominates. For the correlation system the actual improvement is somewhere between the two above extremes, tending toward the higher one at the lower frequencies and vice versa.

V
EXPERIMENTAL STUDIES

5.1 Log Conical Antennas

Two log conical antennas have been assembled and tested with various balun configurations. Only VSWR data has been collected and in general the results are similar to those discussed in the first quarterly report by Sengupta et al (1966). A typical plot of the data is shown in Fig. 12.

The two log conical antennas constructed differed from the previous log conical in that the conductive filaments were fabricated from conventional hook-up wire. If we designate these antennas A and B, the filament of A was No. 16 plastic insulated hook-up wire, and the filament of B was No. 16 uninsulated hook-up wire. Both of these antennas were tested using Duncan-Minerva tapered baluns. The data for antenna B tended to be slightly better and is shown in Fig. 12.

Presently it is felt that it will be difficult to improve the VSWR of the conical antenna much below 3:1/50 ohms without a complex impedance transformation network. To obtain a better insight into the feasibility of matching the conical antenna over a broadband (5:1 or 10:1) to a VSWR of less than 2:1/50 ohms, it will be necessary to obtain additional impedance data. This could best be obtained by the use of a simple narrow band balun configuration that can be tuned to several of the frequencies within the desired band. The impedance obtained at these spot frequencies would be employed in an investigation of matching techniques which would be applicable to obtaining the desired VSWR characteristics ($< 2:1/50$ ohms) for the log conical antenna.

It appears that the log conical antenna is not ideally suited for use on the azimuth elevation directionfinder antenna because of its physical configuration. It is felt, however, that the above impedance study is warranted, since electrically the antenna has some desirable features. Because of the limitations of the log conical antenna for the present application, an order has been placed to obtain a commercially available 10:1 band flat spiral antenna.

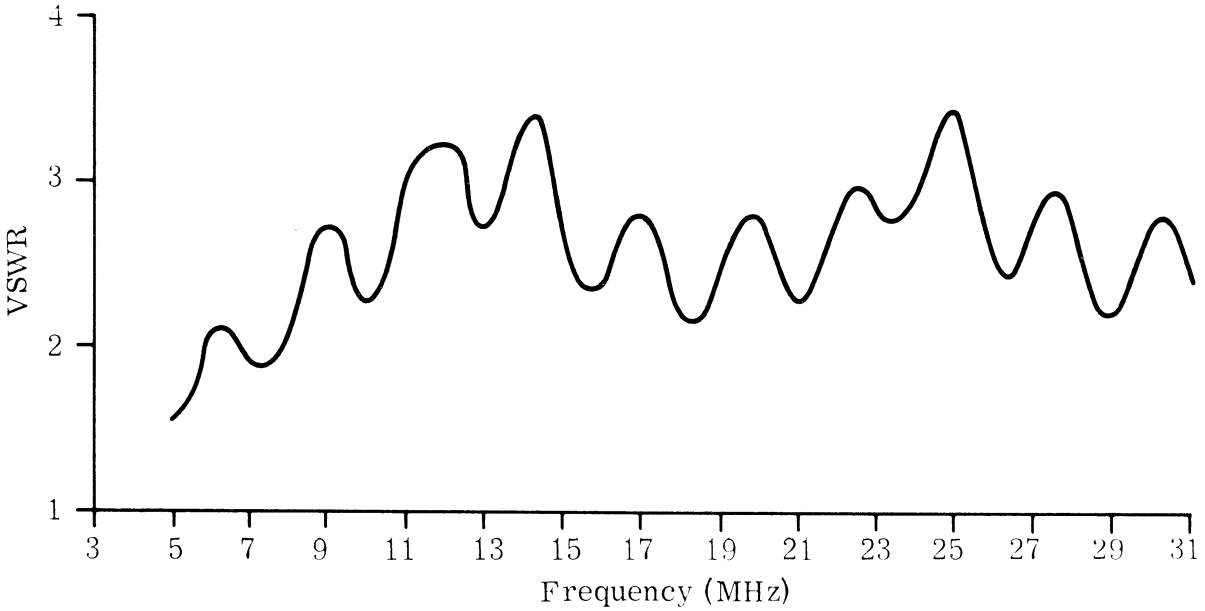

FIG. 12: VSWR CHARACTERISTICS OF LOG CONICAL ANTENNA (B) WITH DUNCAN-MINERVA BALUN

5.2 Development of a Power Divider

An eight-way power divider has been designed, fabricated and tested. The power divider was fabricated from copper clad laminate material (copper clad both sides) and is shown in Figs. 13 and 14. The design is based on strip transmission line theory. The input of the strip transmission line is located at the end with a single connector. To achieve the 8:1 power division, a tapered transition (half-wavelength long at the lowest frequency of interest) is employed. At the input the tapered section is designed to be 50 ohms and the output is designed to be 6.25 ohms. At the 6.25 ohm section of the tapered line, eight 50-ohm arms are attached. A typical set of VSWR data for the 8-way power divider is shown in Fig. 15. This data shows the power divider to have a VSWR of less than 2:1 over a 10:1 band, a performance considered to be satisfactory for the present study.

5.3 Discussion

Because of the problems that are expected to be associated with broadband circularly polarized antenna elements, consideration is being given to the use of narrow band circularly polarized crossed dipole antennas as the elements for an experimental model of a section of the azimuth elevation direction finder. Since the characteristics of circularly polarized crossed dipole antennas are well known, it is felt that a better comparison between experimental and theoretical data can be achieved. Essentially, circularly polarized crossed dipoles consist of two dipoles oriented normal to each other and fed in quadrature. This antenna configuration is relatively simple and is well documented in the literature, and therefore will not be covered in further detail here. The principal advantage of the crossed dipole is its well-behaved electrical characteristics over a relatively narrow band of frequencies.

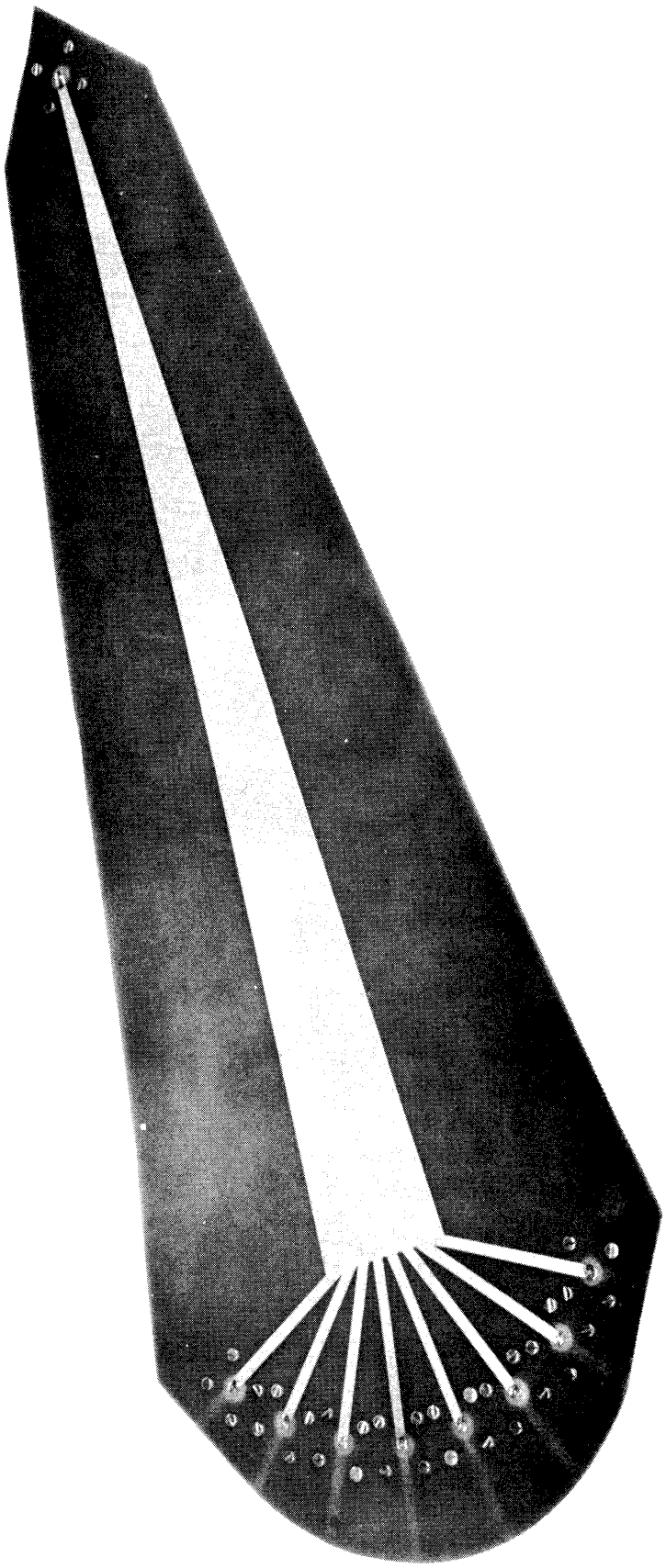

FIG. 13: 8-WAY POWER DIVIDER (PRINTED SIDE)

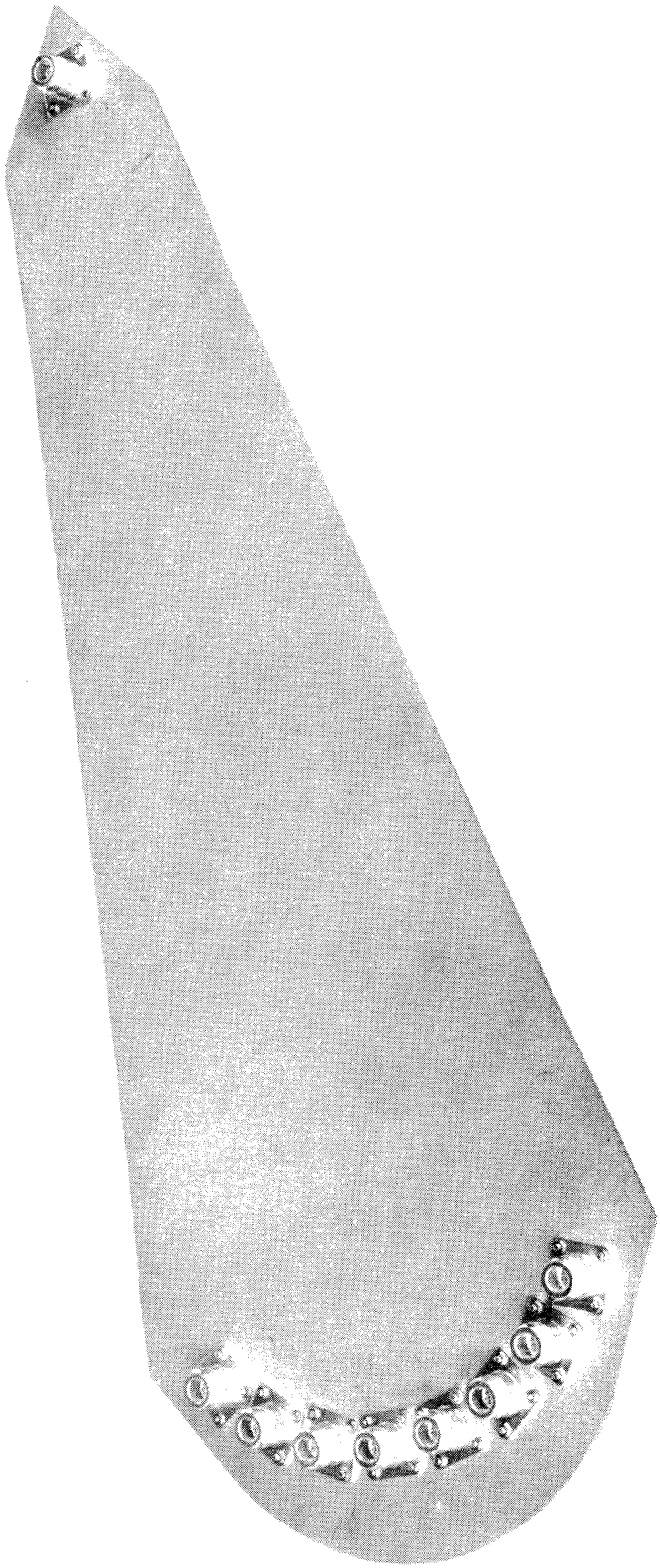

FIG. 14: 8-WAY POWER DIVIDER (TERMINAL SIDE)

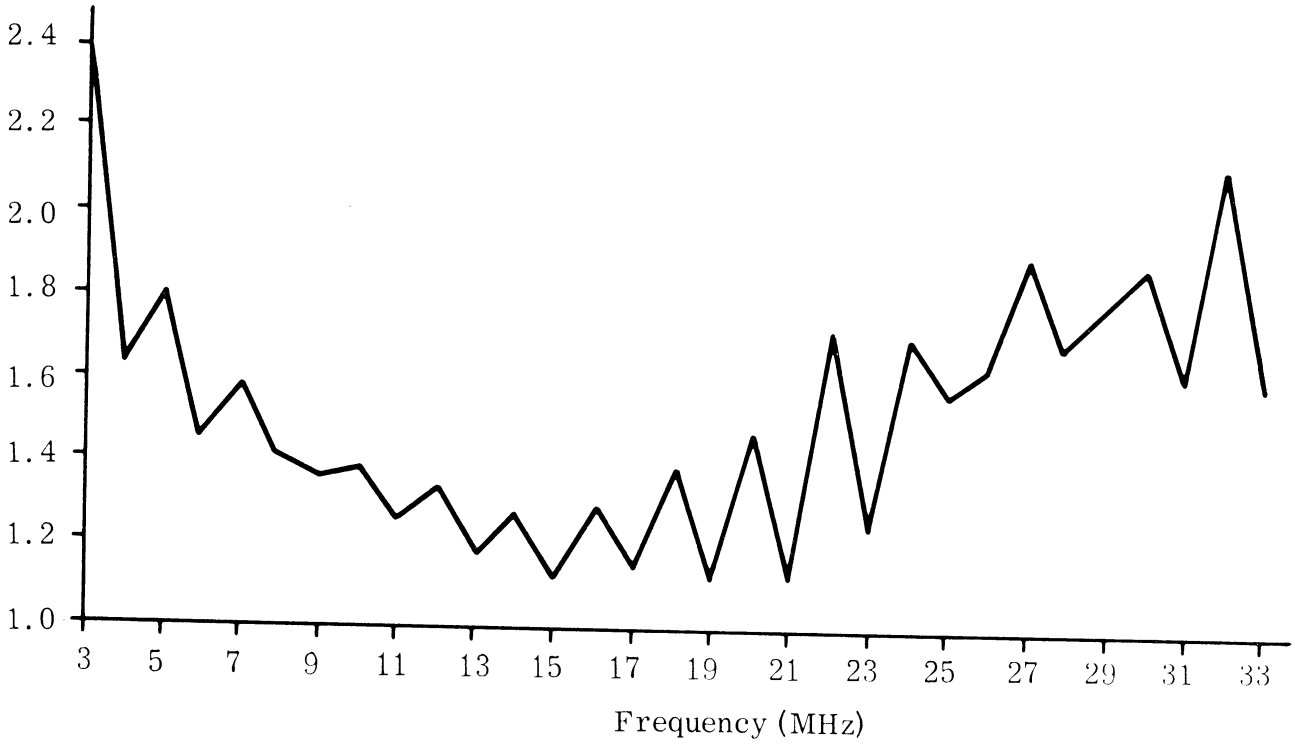

FIG. 15: MICROSTRIP 8-WAY POWER DIVIDER (TERMINAL SIDE)

VI

REFERENCES

Kendall, W. B. (June 1963), "Unambiguous Accuracy of an Interferometer Angle-Measuring System," Trans. IEEE, SET-11, No. 2, pp. 62-70.

Knudsen, H. L. (1956), "Radiation from Ring Quasi-Arrays," Trans. IRE, AP-4, No. 3, pp. 452-472.

Kraus, J. D. (1950), Antennas, McGraw-Hill Book Co., Inc., New York (Ch. II).

Logan, N. A. (Editor) (June 1957), "Diffraction, Reflection and Refraction of Radio Waves, Thirteen Papers by V. A. Fock," AFCRC-TN-57-102, ASTIA Document No. AD 117276 pp. 49-50.

Neff, H. P. and J. D. Tillman (1960), "An Electronically Scanned Circular Antenna Array," IRE Intern. Conv. Record, Pt. 1, 8, pp. 41-47.

Sengupta, D. L., J. E. Ferris, R. W. Larson and T. M. Smith (1965), "Azimuth and Elevation Direction Finder Study" Quarterly Report No. 1, ECOM-01499-1, The University of Michigan Radiation Laboratory Report 7577-1-Q.

Sengupta, D. L. (1966), "Directional Circular Arrays," The University of Michigan Radiation Laboratory Internal Memorandum 07577-509-M.

Woodward, P. M. (1953), Probability and Information Theory with Applications to Radar, Pergamon Press, New York.

	Copies
Commander Aeronautical Systems Division Wright-Patterson AFB, Ohio 45433 Attn: AVWE-3 (Mr. E.M. Turner)	1
Commander A. F. Cambridge Research Laboratory L.G. Hanscom Field Bedford, Massachusetts 01731 Attn: CRD (Mr. C.J. Sletten)	1
Commander Rome Air Development Center Griffiss AFB, New York 13442 Attn: EMATA (Mr. C.L. Pankiewicz)	1
NASA Goddard Space Flight Center Greenbelt, Maryland Attn: Mr. P.A. Lantz, Code 525	1
USAEL Liaison Officer Rome Air Development Center Attn: RAOL Griffiss Air Force Base, New York 13442	1
Director National Security Agency Fort G.G. Meade, Maryland, 20755 Attn: R31 (Mr. J.B. Norvell)	1
Naval Research Laboratory Attn: Dr. R.J. Adams, Code 5330 Washington, D.C. 20390	1
Chief, Bureau of Ships Department of the Navy Main Navy Building Washington, D.C. 20360 Attn: Mr. R. Fratila Code 362A	1

	Copies
Commanding General US Army Electronics Command Attn: AMSEL-HL-R Fort Monmouth, NJ 07703	1
Commander U.S. Navy Electronics Laboratory Attn: Mr. B.I. Small, Code 3220C San Diego, California, 92152	1
Commanding General U.S. Army Security Agency Arlington Hall Station Arlington, Virginia 22207 Attn: IALOG/ESE (Mr. C. Craig)	1
Commanding General U.S. Army Electronics Command Attn: AMSEL-NL-R Fort Monmouth, New Jersey, 07703	1
Defense Documentation Center Attn: DDC-IRE Cameron Station Building 5 Alexandria, Virginia 22314	20
Office of Assistant Secretary of Defense (R and E) Attn: Technical Library Rm 3E1065 Washington D C 20301	1
Defense Intelligence Agency Attn: DIARD Washington, D. C. 20301	1
Bureau of Ships Technical Library Attn: Code 312 Main Navy Building, Room 1528 Washington D. C. 20325	1
Director, U.S. Naval Research Laboratory Attn: Code 2027 Washington D. C. 20390	1

	Copies
Commanding Officer and Director U. S. Navy Electronics Laboratory ATTN: Library San Diego, California 92101	1
AFSC S and T Liaison Officer (RTSND) U S Naval Air Development Center Johnsville Warminster, Pennsylvania 18974	1
Systems Engineering Group SEPIR Wright-Patterson AFB, Ohio 45433	1
Electronic Systems Division AFSC Scientific and Technical Info Div (ESTI) L G Hanscom Field Bedford, Massachusetts 01731	2
Air Force Cambridge Research Laboratories ATTN: CRXL-R L. G. Hanscom Field Bedford, Massachusetts 01731	2
NASA Representative Scientific and Technical Information Facility P. O. Box 5700 Bethesda, Maryland 20014	1
Commanding General U. S. Army Electronics Command ATTN: AMSEL-WL-S Fort Monmouth, New Jersey 07703	5
U. S. Army Electronics Command EW-MET Commodity Attn: AMSEL-EW, Management Office Fort Monmouth, New Jersey 07703	1
U. S. Army Electronics Command ATTN: AMSEL-MR 225 South 18th Street Philadelphia Pennsylvania 19103	1

	Copies
U. S. Army Electronics Command Attn: AMSEL-IO-T Fort Monmouth, New Jersey 07703	1
U. S. Army Electronics Command ATTN: AMSEL-XL-D Fort Monmouth, New Jersey 07703	1
U. S. Army Electronics Command ATTN: AMSEL-RD-MAT Fort Monmouth, New Jersey 07703	1
U. S. Army Electronics Command ATTN: AMSEL-RD-MAF Fort Monmouth, New Jersey 07703	1
U. S Army Electronics Command ATTN: AMSEL-RD-LNA Fort Monmouth, New Jersey 07703	1
U. S. Army Electronics Command ATTN: AMSEL-RD-LNR Fort Monmouth, New Jersey 07703	1
U. S Army Electronics Command R and D Activity ATTN: Commanding Officer White Sands Missile Range, New Mexico 88002	1
U. S. Army Electronics Command ATTN: Chief, Mountain View Office Electronic Warfare Laboratory P. O. Box 205 Mountain View, California 94042	1
U S. Army Electronics Command ATTN: Chief, Intelligence Materiel Development Office Electronic Warfare Laboratory Fort Holabird, Maryland 21219	1
U S. Army Electronics Command Liaison Officer, ASDL-9 Aeronautical Systems Division Wright-Patterson AFB, Ohio 45433	1

	Copies
U.S. Army Electronics Command Liaison Officer, EMPL Roame Air Development Center Griffiss AFB, New York 13442	1
U.S. National Bureau of Standards Boulder Laboratories ATTN: Library Boulder, Colorado 80301	1
Chief of Research and Development Department of the Army Washington, D.C. 20315	2
Office of the Chief of Communications-Electronics ATTN: CCEES-1A Department of the Army Washington, D.C. 20315	1
Commanding General U.S. Army Materiel Command ATTN: R and D Directorate Washington, D.C. 20315	2
Commanding Officer 52D USASASOC Fort Huachuca, Arizona 85613	1
Deputy Commander U.S. Army Combat Developments Command Communications-Electronics Agency Fort Huachuca, Arizona 85613	1
Commanding General, U.S. Army Security Agency ATTN: ACofs, G4 (Technical Library) Arlington Hall Station Arlington, Virginia 22207	2

Commanding Officer
Harry Diamond Laboratories
Connecticut Ave and Van Ness St., N.W.
Washington, D.C. 20438 — 1

Commanding Officer
U.S. Army Engineer R and D Laboratories
ATTN: Stinfo Branch
Fort Belvoir, Virginia 22060 — 1

Commanding General
U.S. Army Electronic Proving Ground
ATTN: Technical Library
Fort Huachuca, Arizona 85613 — 1

Total — 75

UNCLASSIFIED

Security Classification

DOCUMENT CONTROL DATA - R&D

(Security classification of title, body of abstract and indexing annotation must be entered when the overall report is classified)

1. ORIGINATING ACTIVITY *(Corporate author)*
The University of Michigan Radiation Laboratory
Department of Electrical Engineering
Ann Arbor, Michigan 48108

2a. REPORT SECURITY CLASSIFICATION
UNCLASSIFIED

2b GROUP

3. REPORT TITLE
Azimuth and Elevation Direction Finder Study (U)

4. DESCRIPTIVE NOTES *(Type of report and inclusive dates)*
Quarterly Report No. 2 1 December 1965 - 28 February 1966

5. AUTHOR(S) *(Last name, first name, initial)*
Sengupta, Dipak L.; Ferris, Joseph E.; Hok, Gunnar; Larson, Ronal W.; Smith, Thomas M.

6. REPORT DATE	7a. TOTAL NO. OF PAGES	7b. NO. OF REFS
March 1966	42	8

8a. CONTRACT OR GRANT NO.	9a. ORIGINATOR'S REPORT NUMBER(S)
DA 28-043 AMC-01499(E)	7577-2-Q
b. PROJECT NO 5A6 79191 D902 01 04	
c.	9b. OTHER REPORT NO(S) *(Any other numbers that may be assigned this report)*
d.	ECOM-01499-2

10. AVAILABILITY/LIMITATION NOTICES
Each transmittal of this document outside The Department of Defense must have prior approval of USAECOM, AMSEL-WL-S, Fort Monmouth, New Jersey.

11. SUPPLEMENTARY NOTES	12. SPONSORING MILITARY ACTIVITY
	U.S. Army Electronics Command AMSEL-WL-S Fort Monmouth, New Jersey 07703

13. ABSTRACT

The results of numerical computation of the radiation patterns produced by a spherical antenna array are reported. Each antenna element is assumed to produce circularly polarized radiation having a cosine type of pattern. It is found that the pattern stays fairly constant as the beam is steered over the hemisphere. For wide spacing between the elements large subsidiary lobes appear in the pattern. From the calculated patterns an estimate is made about the directivity of the array. Patterns are also calculated for the case when no phasing is introduced in the individual elements.

An approximate method is developed to explain the subsidiary lobes in the pattern produced by a circular array of isotropic elements when the spacing between the adjacent elements is of the order of or larger than a wavelength.

The basic principles of a signal processing method are described which eliminate the use of individual variable phase shifters necessary for steering the beam in conventional antenna arrays.

The results of experimental studies of the log conical spiral antenna and a VHF power dividing circuit are reported.

DD FORM 1 JAN 64 1473

UNCLASSIFIED

Security Classification

14 KEY WORDS	LINK A		LINK B		LINK C	
	ROLE	WT	ROLE	WT	ROLE	WT
ANTENNA ARRAY SPHERICAL ARRAY CIRCULAR ARRAY GRATING LOBES DATA PROCESSING ARRAY						

INSTRUCTIONS

1. ORIGINATING ACTIVITY: Enter the name and address of the contractor, subcontractor, grantee, Department of Defense activity or other organization *(corporate author)* issuing the report.

2*a*. REPORT SECURITY CLASSIFICATION: Enter the overall security classification of the report. Indicate whether "Restricted Data" is included. Marking is to be in accordance with appropriate security regulations.

2*b*. GROUP: Automatic downgrading is specified in DoD Directive 5200.10 and Armed Forces Industrial Manual. Enter the group number. Also, when applicable, show that optional markings have been used for Group 3 and Group 4 as authorized.

3. REPORT TITLE: Enter the complete report title in all capital letters. Titles in all cases should be unclassified. If a meaningful title cannot be selected without classification, show title classification in all capitals in parenthesis immediately following the title.

4. DESCRIPTIVE NOTES: If appropriate, enter the type of report, e.g., interim, progress, summary, annual, or final. Give the inclusive dates when a specific reporting period is covered.

5. AUTHOR(S): Enter the name(s) of author(s) as shown on or in the report. Enter last name, first name, middle initial. If military, show rank and branch of service. The name of the principal author is an absolute minimum requirement.

6. REPORT DATE: Enter the date of the report as day, month, year; or month, year. If more than one date appears on the report, use date of publication.

7*a*. TOTAL NUMBER OF PAGES: The total page count should follow normal pagination procedures, i.e., enter the number of pages containing information.

7*b*. NUMBER OF REFERENCES: Enter the total number of references cited in the report.

8*a*. CONTRACT OR GRANT NUMBER: If appropriate, enter the applicable number of the contract or grant under which the report was written.

8*b*, 8*c*, & 8*d*. PROJECT NUMBER: Enter the appropriate military department identification, such as project number, subproject number, system numbers, task number, etc.

9*a*. ORIGINATOR'S REPORT NUMBER(S): Enter the official report number by which the document will be identified and controlled by the originating activity. This number must be unique to this report.

9*b*. OTHER REPORT NUMBER(S): If the report has been assigned any other report numbers *(either by the originator or by the sponsor)*, also enter this number(s).

10. AVAILABILITY/LIMITATION NOTICES: Enter any limitations on further dissemination of the report, other than those imposed by security classification, using standard statements such as:

(1) "Qualified requesters may obtain copies of this report from DDC."

(2) "Foreign announcement and dissemination of this report by DDC is not authorized."

(3) "U. S. Government agencies may obtain copies of this report directly from DDC. Other qualified DDC users shall request through

_____."

(4) "U. S. military agencies may obtain copies of this report directly from DDC. Other qualified users shall request through

_____."

(5) "All distribution of this report is controlled. Qualified DDC users shall request through

_____."

If the report has been furnished to the Office of Technical Services, Department of Commerce, for sale to the public, indicate this fact and enter the price, if known.

11. SUPPLEMENTARY NOTES: Use for additional explanatory notes.

12. SPONSORING MILITARY ACTIVITY: Enter the name of the departmental project office or laboratory sponsoring *(paying for)* the research and development. Include address.

13. ABSTRACT: Enter an abstract giving a brief and factual summary of the document indicative of the report, even though it may also appear elsewhere in the body of the technical report. If additional space is required, a continuation sheet shall be attached.

It is highly desirable that the abstract of classified reports be unclassified. Each paragraph of the abstract shall end with an indication of the military security classification of the information in the paragraph, represented as *(TS)*, *(S)*, *(C)*, or *(U)*

There is no limitation on the length of the abstract. However, the suggested length is from 150 to 225 words.

14. KEY WORDS: Key words are technically meaningful terms or short phrases that characterize a report and may be used as index entries for cataloging the report. Key words must be selected so that no security classification is required. Identifiers, such as equipment model designation, trade name, military project code name, geographic location, may be used as key words but will be followed by an indication of technical context. The assignment of links, rules, and weights is optional.